Award Number: W81XWH-09-2-0188

TITLE: Facial Fracture Risk Functions for Assessing the Performance of Improved Face and Eye Protective Equipment

PRINCIPAL INVESTIGATOR: Mr. Frederick Brozoski

CONTRACTING ORGANIZATION: The Geneva Foundation
Tacoma, WA 98402-4437

REPORT DATE: September 2012

TYPE OF REPORT: Final

PREPARED FOR: U.S. Army Medical Research and Materiel Command
Fort Detrick, Maryland 21702-5012

REPORT DOCUMENTATION PAGE

Form Approved
OMB No. 0704-0188

1. REPORT DATE	**2. REPORT TYPE**	**3. DATES COVERED**
September 2012	Final	29 September 2009 - 28 August 2012

4. TITLE AND SUBTITLE
Facial Fracture Risk Functions for Assessing the Performance of Improved Face and Eye Protective Equipment

5a. CONTRACT NUMBER

5b. GRANT NUMBER
W81XWH-09-2-0188

5c. PROGRAM ELEMENT NUMBER

6. AUTHOR(S)
Mr. Frederick Brozoski

E-Mail: krobinson@genevausa.org

5d. PROJECT NUMBER

5e. TASK NUMBER

5f. WORK UNIT NUMBER

7. PERFORMING ORGANIZATION NAME(S) AND ADDRESS(ES)
The Geneva Foundation
Tacoma, WA 98402-4437

8. PERFORMING ORGANIZATION REPORT NUMBER

9. SPONSORING / MONITORING AGENCY NAME(S) AND ADDRESS(ES)
U.S. Army Medical Research and Materiel Command
Fort Detrick, Maryland 21702-5012

10. SPONSOR/MONITOR'S ACRONYM(S)

11. SPONSOR/MONITOR'S REPORT NUMBER(S)

12. DISTRIBUTION / AVAILABILITY STATEMENT
Approved for Public Release; Distribution Unlimited

13. SUPPLEMENTARY NOTES

14. ABSTRACT
The reduction in structural failures of the facial bones is of extreme importance because of the protective characteristics of the facial bones. This reduction can lead to a reduction in injuries to both the brain and the eye. This report describes a focused effort to determine the tolerance thresholds of facial bones subjected to blunt impact in the lateral direction. A total of 64 tests were performed in the lateral direction using a free-falling mass. Acoustic emission sensors were used to detect the onset of fracture to produce non-censored fracture data. Injury risk functions for blunt lateral impact have been developed for the frontal, zygoma, and nasal bones. Furthermore, a series of 22 matched tests were performed to access the biofidelic and repeatable response for lateral impact to the frontal, zygoma, and nasal bones. Future use of these analyses will aid design engineers in optimizing the development of enhanced face and eye protective equipment.

15. SUBJECT TERMS- none provided

16. SECURITY CLASSIFICATION OF:			**17. LIMITATION OF ABSTRACT**	**18. NUMBER OF PAGES**	**19a. NAME OF RESPONSIBLE PERSON**
					USAMRMC
a. REPORT	**b. ABSTRACT**	**c. THIS PAGE**			**19b. TELEPHONE NUMBER** *(include area code)*
U	U	U	UU	41	

Table of Contents

INTRODUCTION: The reduction in structural failures of the facial bones is of extreme importance because of the protective characteristics of the facial bones. This reduction can lead to a reduction in injuries to both the brain and the eye. Based on the types of injuries sustained in military situations, countermeasures such as helmets, goggles and facemasks can be designed to effectively distribute loads to reduce the incidence of injuries. In order to design the protective equipment, the local injury thresholds for the facials bones must be developed. A useful tool to measure the effectiveness of the current countermeasures is the FOCUS headform, but injury criteria is needed to correlate injury risk from lateral impact to the measured response of the advanced headform (Figure 1). The FOCUS headform has the ability to measure forces applied to the facial and orbital structures. It has been developed by Virginia Tech and Denton ATD and validated for eye injury prediction. The headform is comprised of eight separate sensing regions within the facial structures that overlie embedded load cells. These regions correspond to the frontal bone, nasal bone, zygoma, maxilla and mandible. Each "bone" or reaction surface is made of a rigid urethane plastic that is attached to a load cell which is supported by an internal aluminum frame. The outer skin, eyes and nose insert are made of a soft urethane. Each load cell is capable of measuring forces in three axes. Facial fracture experimental impact testing is needed to better characterize facial fracture injury risk. Therefore, the first goal of this study was to perform tests with post mortem human surrogates (PMHS) to determine facial fracture injury risk functions for lateral impacts to the zygoma, frontal and nasal bones for the 50th percentile male. The second goal of this study was to demonstrate the response of the FOCUS headform to lateral impacts and assess its biofidelity using corridors developed from the PMHS data.

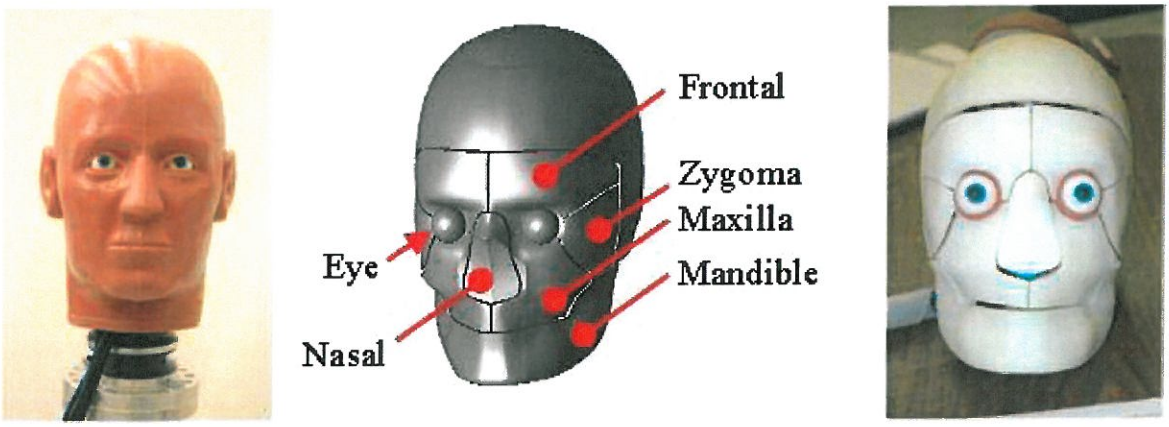

Figure 1: Individual skull segments are shown for the FOCUS headform.

BODY: A total of 64 impact tests were conducted on 20 fresh frozen male PMHS heads using the test setup shown in Figure 2. A 3.18 kg impacting mass was dropped onto the lateral aspects of the zygoma, frontal, and nasal bone. The PMHS heads were thawed and brought to room temperature prior to testing, and all skin and tissues surrounding the bones were left intact. To create the rigid support for the head, Bondo (polyester resin

that hardens when mixed with a catalyst) was poured around the head and three screws were drilled through the support into the head to eliminate relative motion between the head and support. A separate drop height was used for each of the three bones in order to ensure fracture, and only one impact per bone per head was performed. The impacting surface had an area of 6.5 cm^2 and was machined with a slight bevel around its surface to reduce edge effects. A high speed video camera was utilized to capture the event to identify the time of impact to aid in the calculation of force deflection. Video data was taken at 2000 frames per second with a resolution of 576 x 576. All subjects were screened for any pre-existing skull fractures or related trauma.

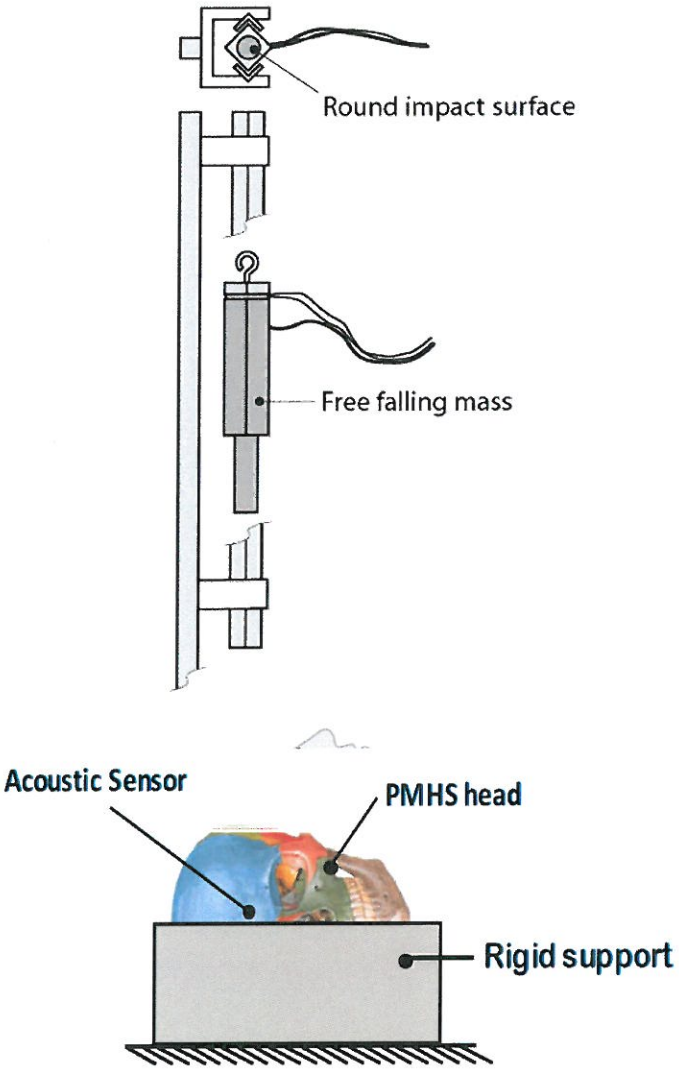

Figure 2: Schematic of test apparatus and instrumentation used for the PHMS tests.

Table 1 displays the drop heights and energies associated with fracture for each bone tested. In addition, non-fracture tests were performed on the frontal bone of 4 heads. The non-fracture tests will be used to help verify fracture thresholds.

Table 1: Drop heights and associated impact energies for each facial bone

Bone	Drop height (cm)	Energy (J)	Fracture Test?
Frontal	5.1	1.6	No
Frontal	152.4	47.5	Yes
Nasal	25.4	7.9	Yes
Zygoma	88.9	27.7	Yes

The impacted side of the head was varied, in which 10 heads were impacted on the right side and 10 heads were impacted on the left side. Furthermore, the order in which the bones were fractured was also varied. The frontal bone was always fractured first, as it does not affect the structural integrity of the nasal or zygoma bones. However, the zygoma was fractured prior to fracturing the nasal bone for 10 heads, and the nasal bone was fractured prior to fracturing the zygoma for 10 heads. This was done so that any potential interaction effects could be quantified. Figure 3 displays the impact locations for each facial bone.

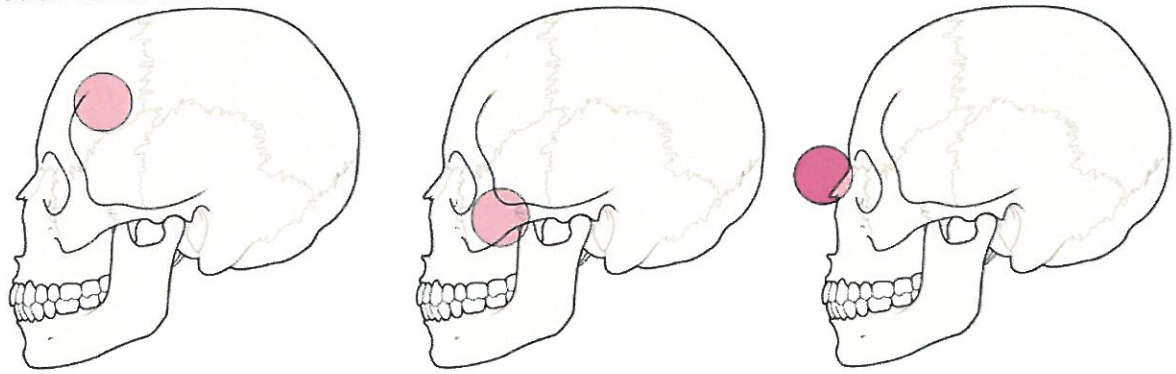

Figure 3: Impact locations for the frontal bone (left), zygoma (center), and nasal bone (right).

The free falling impacting mass was instrumented with two accelerometers at the top (2,000 g, Endevco 7264, San Juan Capistrano CA) of the impactor to allow for inertial compensation of the load cell (4,000 N, Denton Inc, Milan OH) that is positioned on the impacting end (Figure 2). The accelerometer and load cell data was acquired at 20,000 Hz. In addition to the impactor instrumentation, each head was instrumented with Acoustic Emission (AE) sensors (Micro30S, Physical Instruments, New Jersey) sampled at 5,000,000 Hz. The acoustic sensors were mounted directly to the bone by removing the soft tissue and periosteum and gluing the sensor in place with cyanoacrylate adhesive (Figure 4). The acoustic sensor was placed on the frontal bone of each head. The acoustic sensor data allow for the collection of uncensored data which provides much

more accurate injury risk functions. In other words, the acoustic sensor provides the exact timing of fracture so that the exact force value at the time of fracture can be used (Figure 5) (Cormier, 2008). This eliminates errors from using the peak force when fracture occurs well before the peak.

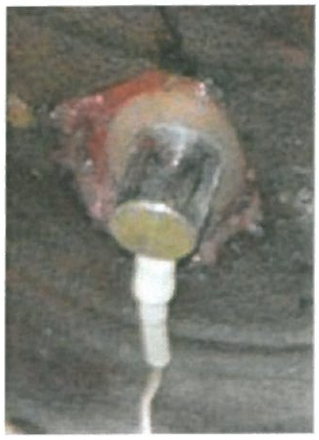

Figure 4: Illustration of acoustic sensor mounted to facial bone.

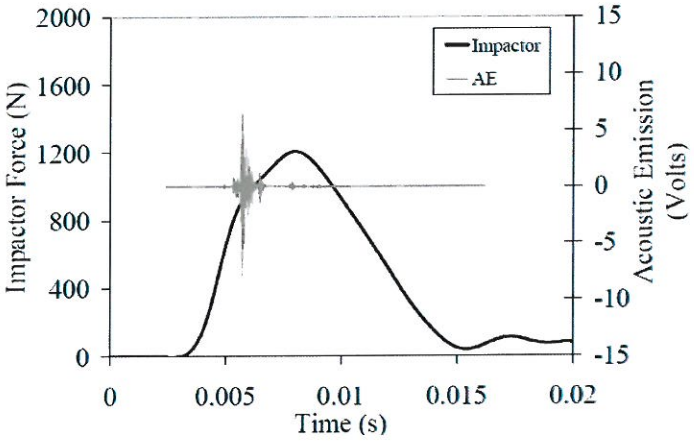

Figure 5: Impactor force and acoustic emission for facial fracture timing during impact.

The exact timing of the acoustic emission event is essential for determining non-censored force valves and therefore a timed output module (TOM) (TOM, DTS Inc, Seal Beach CA) was used in conjunction with the high rate data acquisition system (TDAS, DTS Inc, Seal Beach CA) to ensure an accurate trigger correlation. To utilize acoustic data as a method of estimating the time at which fracture begins, a threshold must be established that differentiates normal background emissions from those associated with the fracture event. This was established in previous test series by examining the maximum voltage of the AE signal as well as the number of counts above a given threshold (Cormier, 2008). The threshold voltage was defined to be 5 Volts for all bones. In this study, fracture force is defined as the first point at which the AE signal reaches 5 Volts.

In order to recreate the position of the impact relative to the external facial geometry for future modeling and data analysis, a laser scan (Platinum Scanner, FARO Technologies, Lake Mary, FL) of the face was taken prior to each test (Figure 6). Along with the Faro Arm scan of the impact location, Computed Tomography (CT) scans of the PMHS heads were performed before and after the experimental testing (Figure 7). The CT imaging provides detailed internal geometries that will be useful for data analysis and quantifying subject variation.

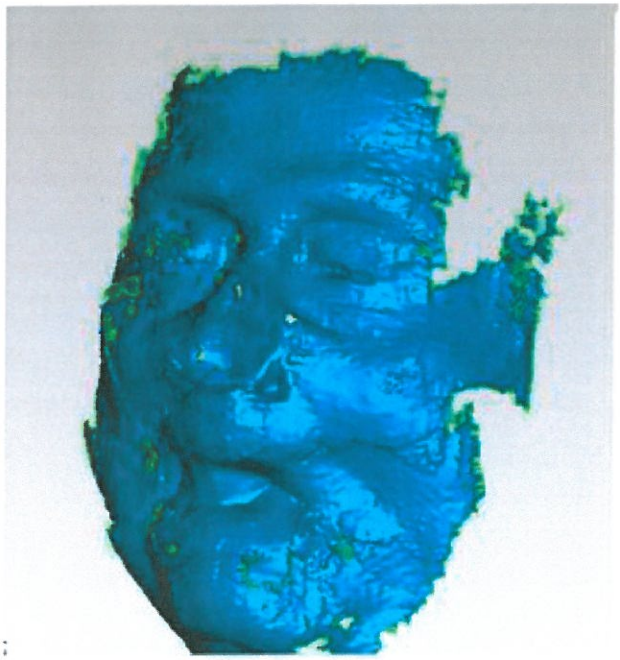

Figure 6: Laser scan of PMHS face to Provide surface geometry

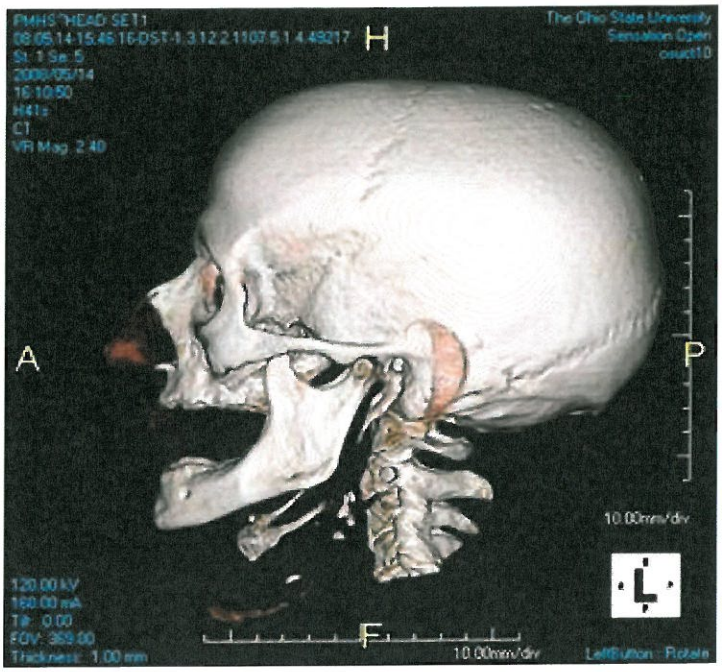

Figure 7: Illustration of PMHS head CT scan showing subject specific skull Geometry.

For each facial bone tested, survival analyses were performed to determine the relationship between fracture force and the risk of fracture for the sample of specimens tested. A parametric approach was used using a Weibull model and was implemented using SAS (SAS Institute, Cary N.C). The Weibull model will account for the non-censored nature of the data used in the analysis to determine the model parameters (Cantor, 2003; Kleinbaum, 2005). Subject age was also included as covariates to assess their potential for predicting the risk of fracture. The Weibull CDF is given by,

$$CDF = 1 - \exp -(\lambda \cdot F)^{\gamma} \quad \textbf{(Equation 1)}$$

Where, λ and γ are the scale and shape parameters, respectively, and F is the applied force. This function will provide an estimate of risk of injury using the maximum likelihood estimates of the scale and shape parameters. A non-parametric model was also created using the Kaplan-Meier method. The Kaplan-Meier method assumes the data are only right or non-censored and determines the risk of fracture based on the number of subjects at risk which sustain a fracture for a given force (Kleinbaum, 2005).

Furthermore, the high-speed video was used to select tests that did not exhibit slippage of the impactor with respect to the skull and would be useful for characterizing the force-displacement response. To define the average force-displacement response of each

bone, a corridor was created to encompass the overall force-displacement response. The response corridor was determined by the mean and standard deviation of the characteristic average (Lessley, 2004). The characteristic average was created using the force-displacement response up to 90% of peak force.

FOCUS Testing

The data provided within this report were obtained by performing blunt lateral impacts using the FOCUS headform. The impacted region included the frontal, nasal and zygoma bones (Figure 8). The impactor was dropped from a height of 8 or 10 inches (20 or 25 cm).

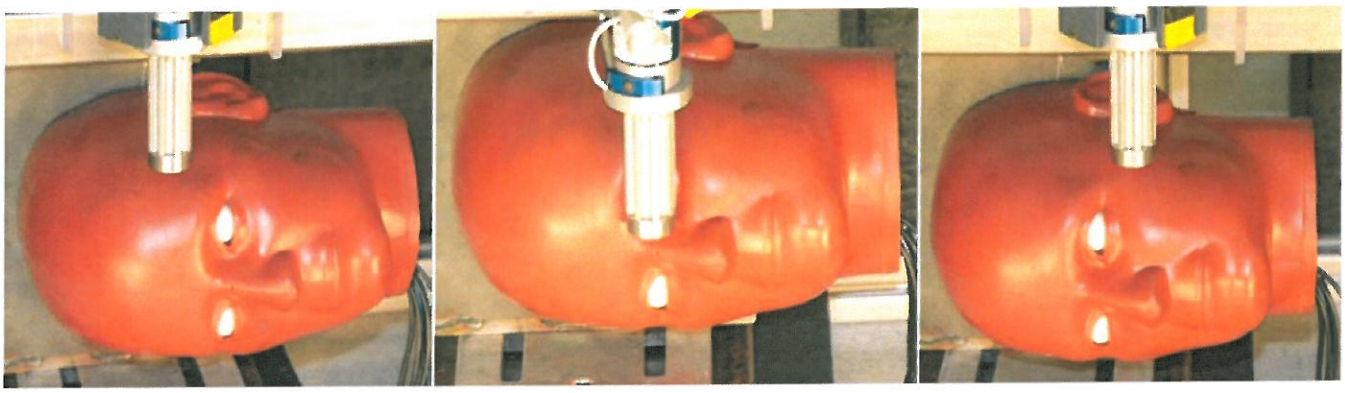

Figure 8: Impactor position for frontal (left), nasal (center) and zygoma (right) impacts.

A series of impacts were performed on corresponding regions of the FOCUS headform in order to characterize its response to blunt impact. Impact severity was chosen to facilitate comparison with cadaver results and to minimize risk of damaging the headform. The impact was applied using the same apparatus and instrumentation scheme used for the cadaver impacts. Each impact was performed using a cylindrical, free-falling rigid aluminum impactor (3.2 kg) with a steel tip. The flat impacting surface had an area of 6.45 cm_2 (1 in_2) and was machined with a slight bevel to reduce edge effects. The rigid impactor was instrumented with three single-axis accelerometers (Endevco 7264B-2000, Endevco Corp., San Juan Capistrano CA). All data were filtered to CFC 300. Impactor displacement was calculated by double-integrating the acceleration data. This displacement data were then used to determine the force-displacement or stiffness response of each impacted region.

The cadaver data utilized as a comparison has been reported previously under separate reports. The previous tests resulted in several force-displacement responses for the frontal, nasal and zygoma regions. Corridors were created which encompass the standard deviation of the cadaver force-displacement response. These corridors will be used in the current report to compare with the FOCUS response data.

RESULTS: A total of 64 impact tests were conducted on 20 fresh frozen male PMHS heads. Data were collected from 2 accelerometers and load cell on the impactor, as well as an acoustic sensor mounted on the frontal bone of each PMHS head. Results for each facial bone are presented individually.

FRONTAL BONE: A total of 24 lateral impacts were performed using male cadaver specimens (Table 2). Fracture did not occur during the four low energy impacts (1.5 J) used to characterize the AE signal as well as two of the high energy (›50J) impacts. The average fracture force was 1994 N (Standard Deviation: 909 N) and the average peak force was 4056 N (SD: 2126) (Figure 9). A threshold for the Acoustic Emission (AE) data associated with fracture was set to 5 volts. This threshold was higher than the maximum value of AE recorded during the non-fracture tests (0.6 v) and was higher than the AE which occurred briefly before the maximum AE was reached. The fracture tests has an average peak AE of 8.7 volts. On average, fracture force was equal to 46% of the peak force achieved during a fracture test (Figure 10). Tests with an average impactor energy of 50 J produced fracture in 17 of 19 subjects. The two subjects that did not sustain a fracture were exposed to peak forces of 8886 and 7506 N.

Table 2: Results of lateral frontal bone impact tests.

Specimen Number	Impact Velocity (m/s)	Impact Energy (J)	Peak Force (N)	Fracture Force (N)
39	0.9	1.2	1112	
39	4.1	26.4	5632	2392
40	0.9	1.4	901	
40	5.7	50.6	3452	1382
41	1.0	1.7	352	
41	5.5	48.1	2710	664
42	0.8	1.1	720	
42	5.5	47.0	5068	2709
43	5.6	49.6	1753	1073
44	5.5	48.2	4413	1783
45	6.2	60.5	7506	
46	5.6	49.6	5409	2206
47	6.4	64.3	4483	710
48	6.3	62.8	3733	1703
49	5.5	48.0	6937	3870
50	5.7	51.4	4169	1502
51	5.9	54.3	4569	3461
52	5.6	49.6	3028	1464
53	5.5	48.6	3753	1172
54	5.7	50.9	5039	2872
55	5.7	51.4	4819	1719
56	5.8	53.4	8886	
57	6.4	63.7	4935	2830
58	5.6	50.2	3963	2380

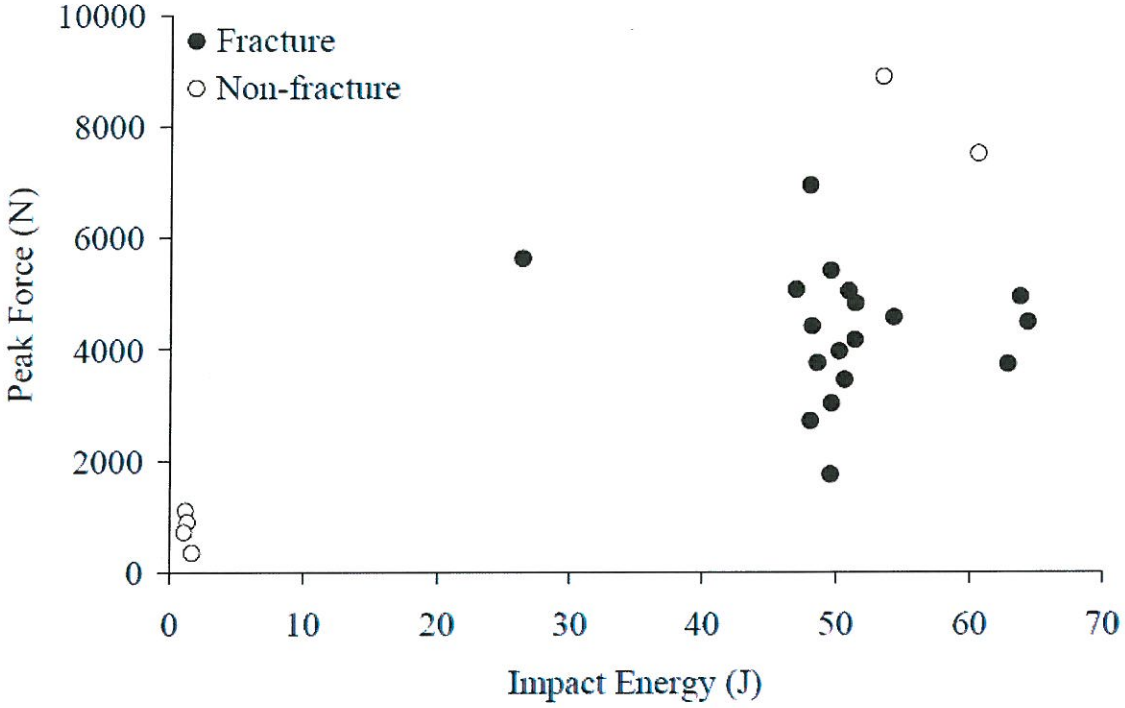

Figure 9: Peak force achieved by fracture status.

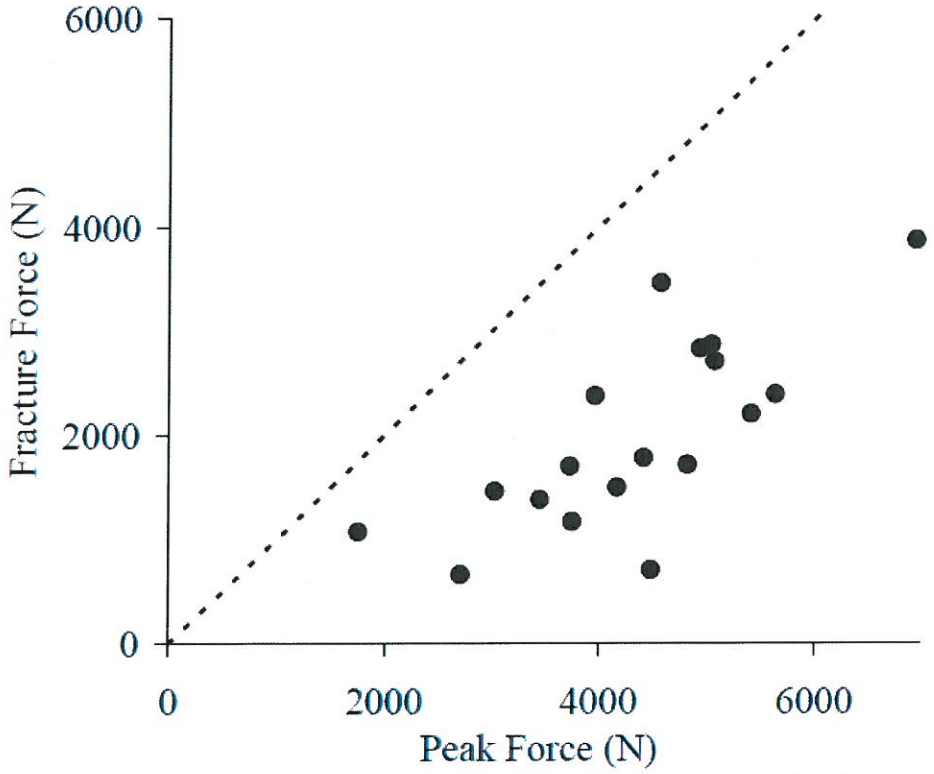

Figure 10: Relationship between peak and fracture force identified using AE data.

The lateral frontal bone impacts had an average pulse duration of 12 ms. A few of the tests contained a single peak in the force response (Figure 11); however, the majority of the tests contained multiple peaks within the force data (Figure 14). Differences in the force displacement response were correlated with the resulting fracture. Tests resulting in lower impactor dispacement (Figure 12) created non-depressed radiating fractures (Figure 13). In comparison, depressed and comminuted fractures (Figure 16) resulted in more extensive impactor motion due to the deeper penetration (Figure 15). The inferior portion of the fracture lines tended to follow the inferor temporal line. Fractures resulting in depression of the skill tended to exhibit radiating fractures to a lesser extent.

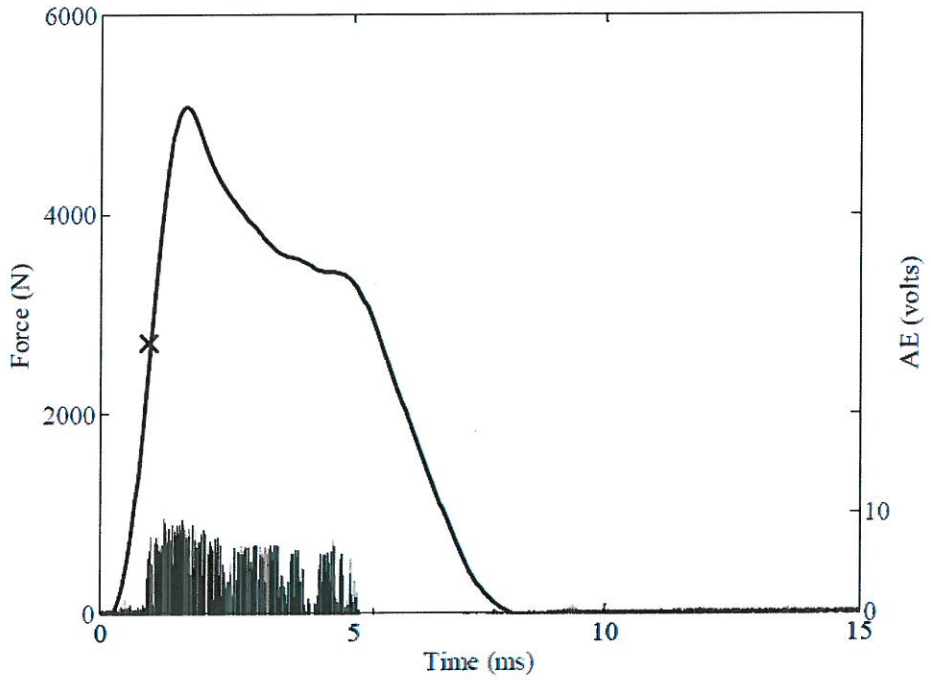

Figure 11: Subject 42 fracture producing impact with AE.

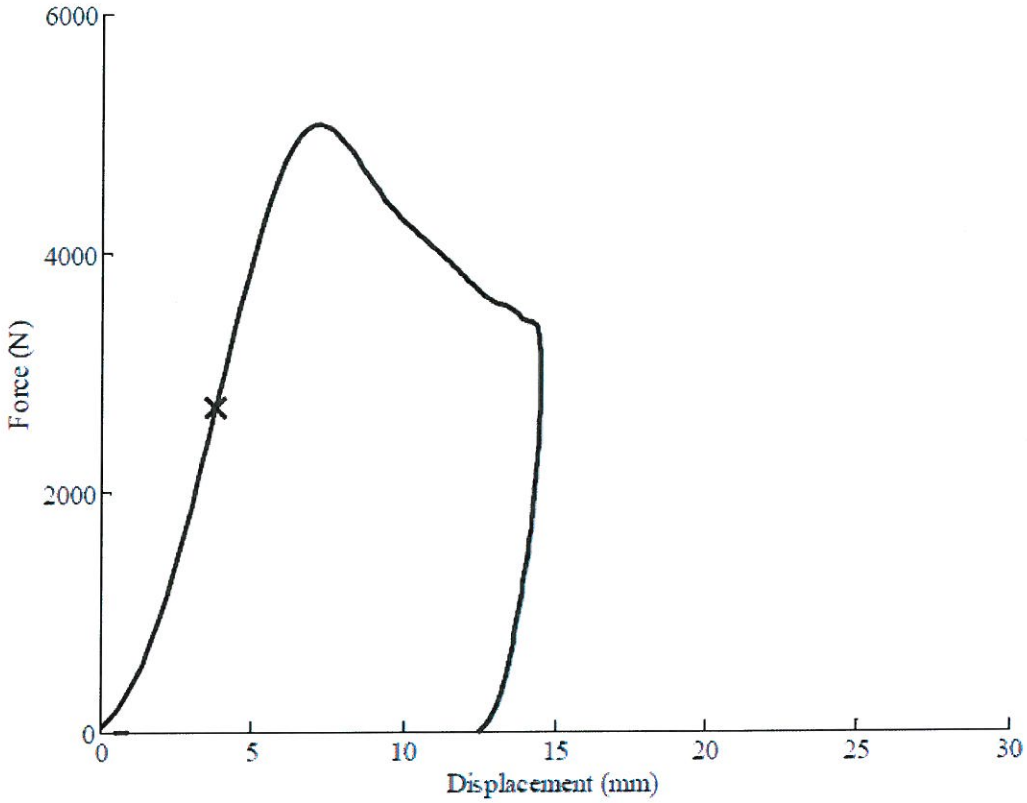

Figure 12: Subject 42 fracture producing impact force-displacement response ("X" denotes force at fracture).

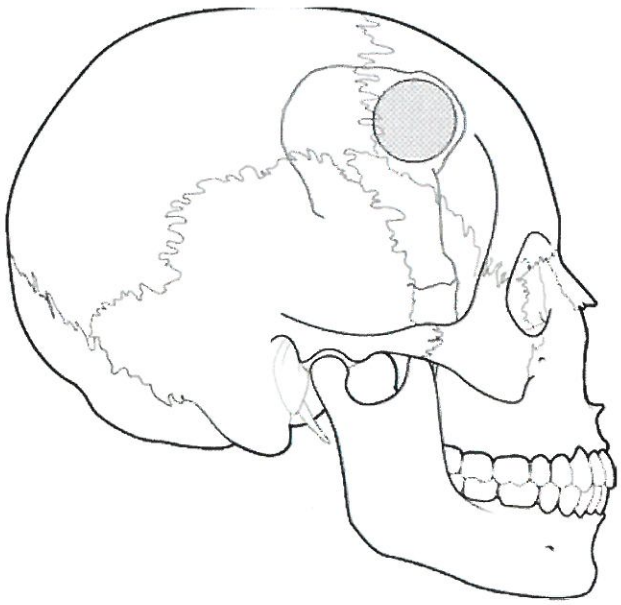

Figure 13: Frontal bone fracture pattern and impact location for subject 42 (same as Figure 11 and Figure 12).

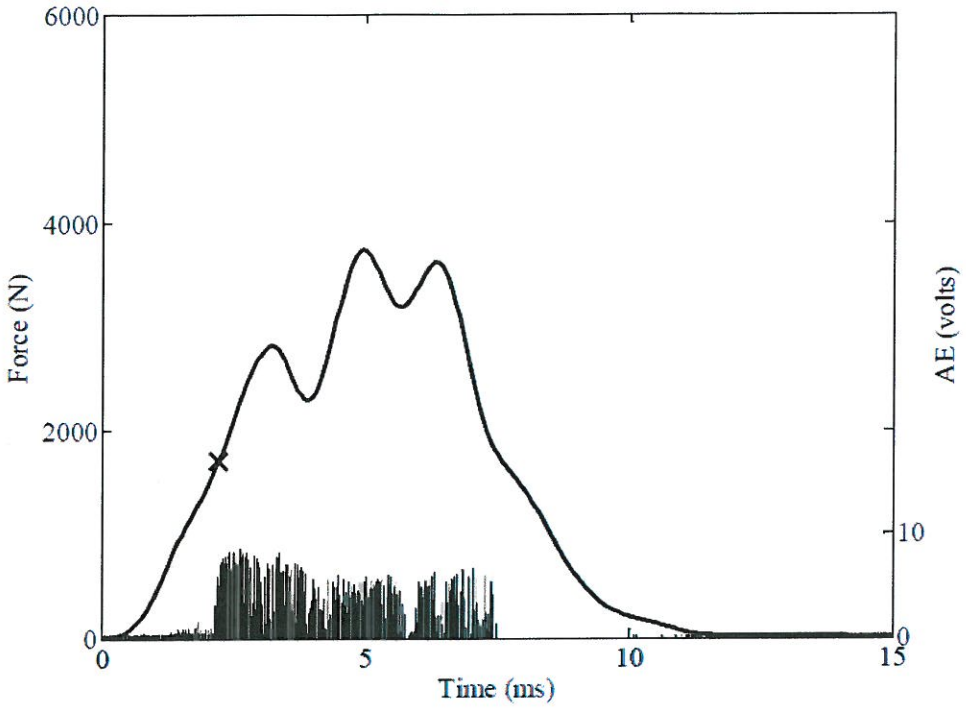

Figure 14: Subject 48 fracture producing impact with AE.

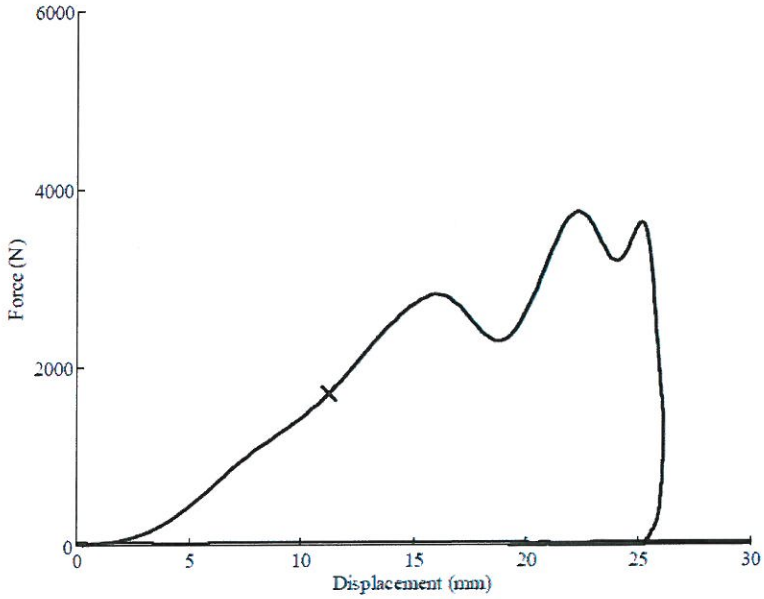

Figure 15: Subject 48 fracture producing impact force-displacement response ("X" denotes force at fracture).

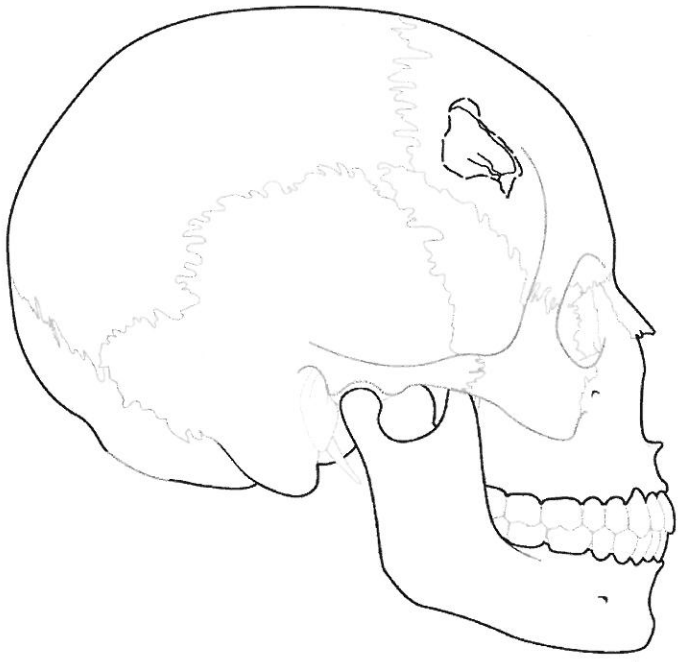

Figure 16: Frontal bone fracture pattern for subject 48 (same as Figures 14 and 15).

The high speed video was used to select tests that did not exhibit slippage of the impactor with respect to the skull and would be useful for characterizing the force-displacement response. Sixteen tests were selected to be used in developing a stiffness corridor to describe the average response of the frontal bone (Figure 17). The average maximum displacement achieved during the corridor tests was 18mm (SD:9).

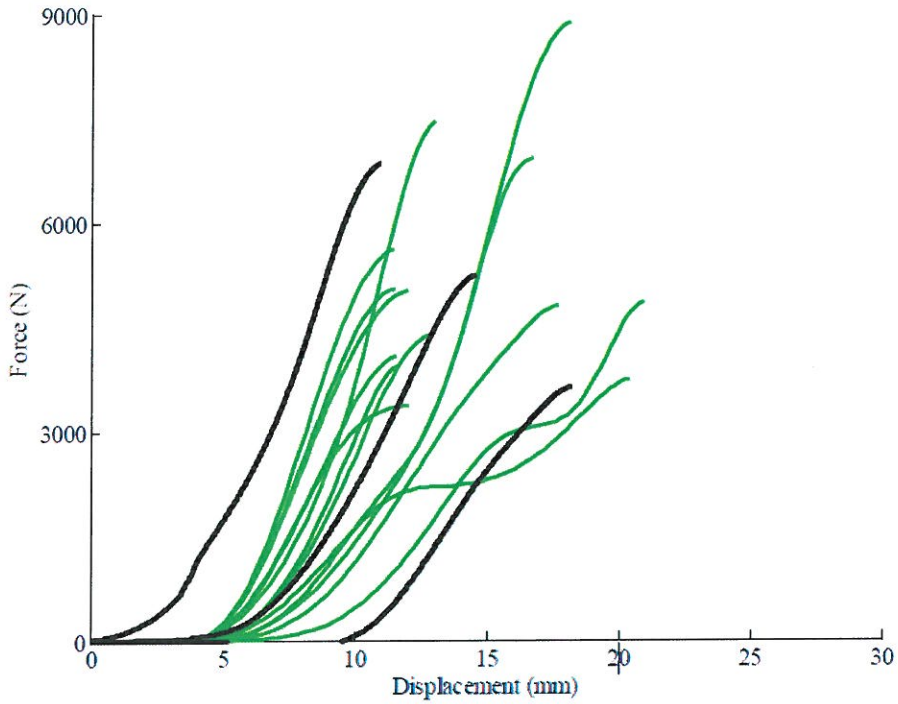

Figure 17: Frontal bone response and corresponding average corridor response and standard deviation.

The risk of fracture was estimated using a Weibull distribution (Table 3) and the Kaplan-Meier non-parametric technique. Both models predict similar risk values up to the 50% risk level. Beyond the 50% risk level, the Kaplan-Meier estimate predicts a higher level of risk than the Weibull model. Age was found to be a statistically significant factor in the risk of frontal bone fracture. For a 10 year increase in age between 70 and 80 years, the force necessary to create a 50% risk of fracture decreases by approximately 1000 N (3000 N vs. 2000 N) (Figure 18). The Weibull survival function is given using equation 2.

Table 3: Parameter estimates for Weibull model.

		95% Confidence Interval	
Parameter	**Estimate**	**Lower**	**Upper**
Intercept	11.07	8.58	13.56
Shape (γ)	1.63	1.16	2.30
Age	1.07	1.18	1.01

$$S = 1 - \exp(-\exp(-\gamma(Intercept + Age\beta_{age})Force^{\gamma} \qquad \text{(Equation 2)}$$

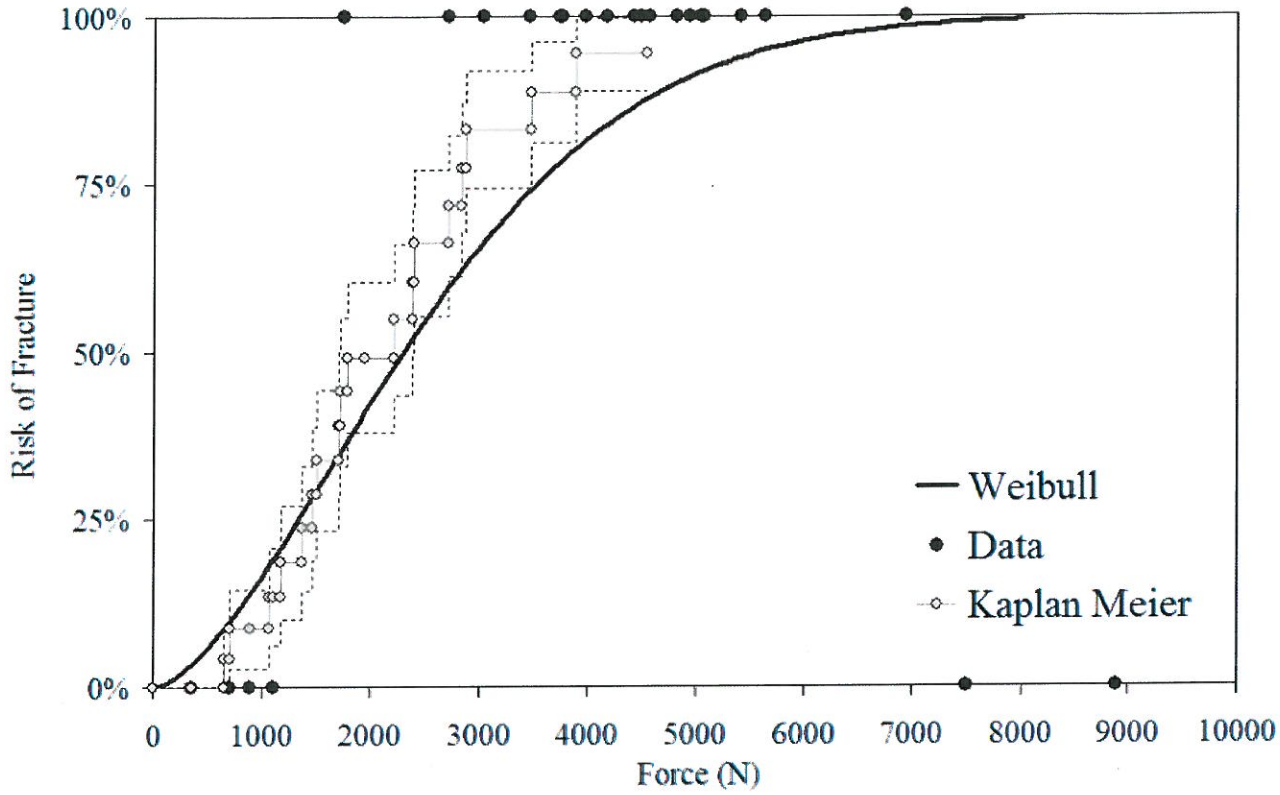

Figure 18: Risk of frontal bone fracture due to lateral impact.

ZYGOMA: A total of 17 lateral impact tests were performed using male cadaver specimens (Table 4). The average impact velocity was 4 m/s which corresponded to an impactor energy of 22 to 33 J with an average of 29 J. Peak force during the zygoma impacts ranged from 913 to 2835 N with an average of 495 N. All 17 tests resulted in a fracture with an average fracture force of 906 N. A threshold for the Acoustic Emission (AE) data associated with fracture was set to 5 volts. The maximum AE measured during fracture producing impacts for the zygoma and frontal bone impacts had an average value of 8.2 and 8.7 respectively. On average, fracture force was equal to 60% of the peak force achieved during the fracture tests (Figure 19). Frequently, the fracture occurred near a deviation in force resulting in a local peak. On average, the fracture force was approximately 77% of the local peak force. Fracture force did not demonstrate a relationship with impactor energy (Figure 20).

Table 4: Results of lateral zygoma impacts.

Specimen Number	Impact Velocity (m/s)	Impact Energy (J)	Peak Force (N)	Fracture Force (N)
39	4.4	31.2	1257	579
40	4.3	28.7	1030	563
41	3.8	22.4	1295	504
42	4.4	30.1	1741	603
43	3.9	24.4	1221	560
44	4.4	30.7	1743	1238
45	4.1	26.8	2021	1301
46	4.3	29.3	2204	1479
49	4.1	27.0	1777	928
50	4.2	27.9	947	898
51	4.2	28.4	1343	860
52	4.4	31.0	1417	656
53	4.2	27.4	1568	553
54	4.6	32.7	913	511
55	4.3	29.5	1424	697
56	4.5	31.6	2835	2792
58	4.4	30.2	1198	673

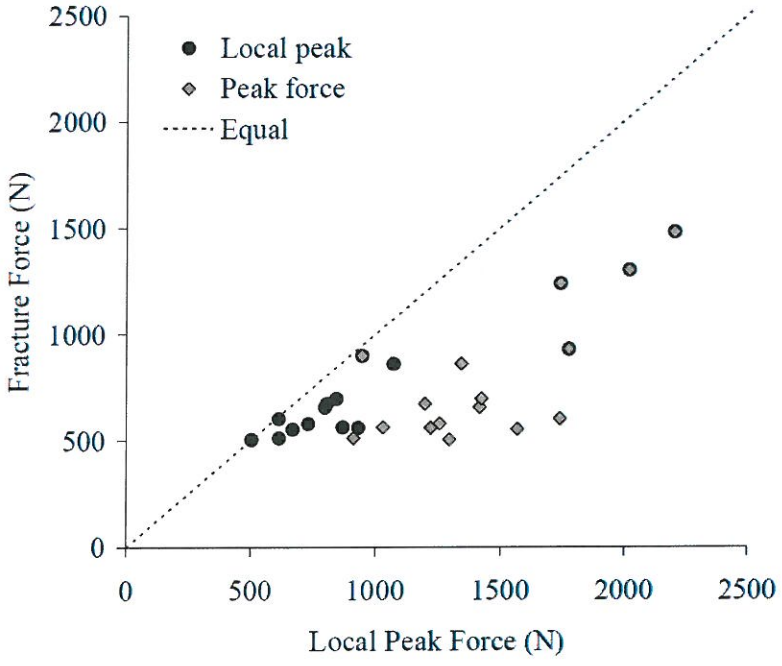

Figure 19: Relationship between peak, local peak and fracture forces.

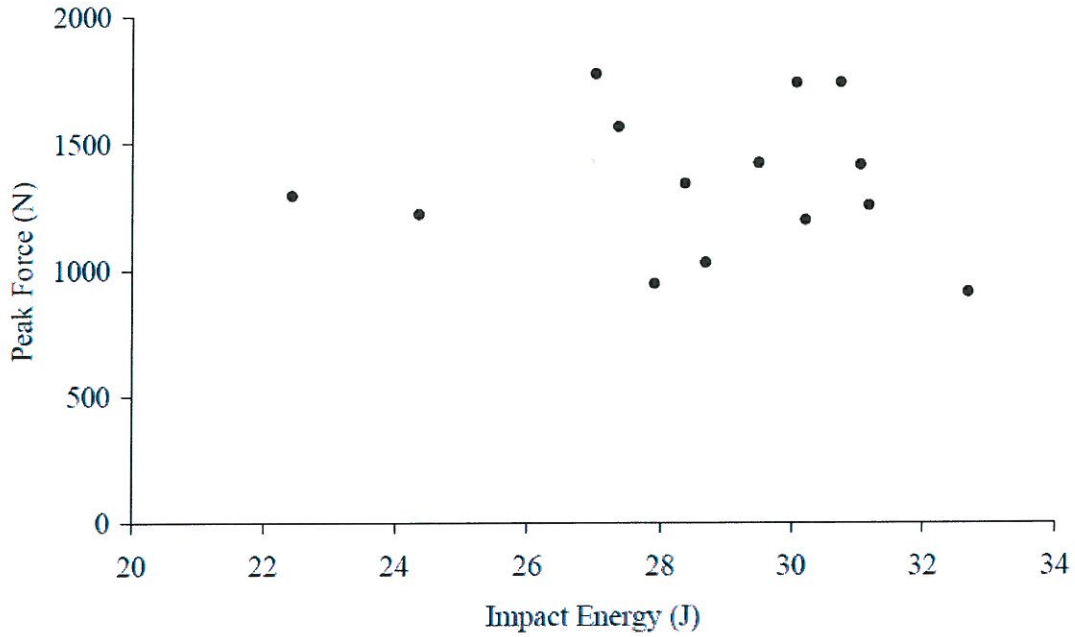

Figure 20: Impactor energy at impact and peak force.

The occurrence of fracture near a local peak was observed in both the force-time and force-displacement responses (Figure 21, Figure 22). In the remaining tests, fracture occurred prior to peak force without a deviation in force prior to the peak (Figure 23, Figure 24). On average, the difference between fracture force and a local peak force was 90 N. After impactor contact, fracture was identified at 5 to 14 mm of displacement with an average of 7 mm.

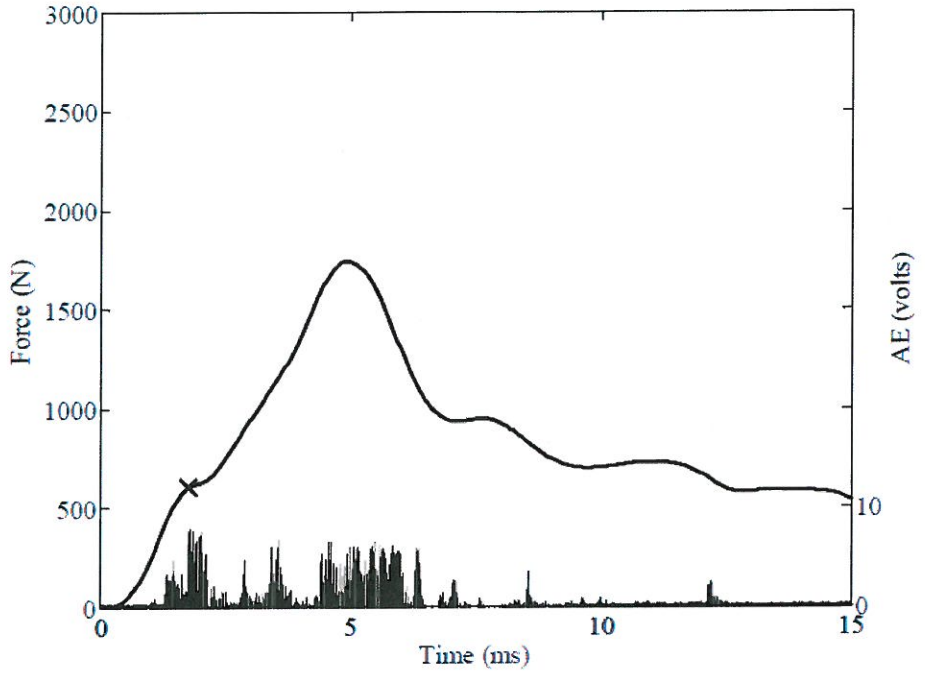

Figure 22: Subject 42 force-displacement response.

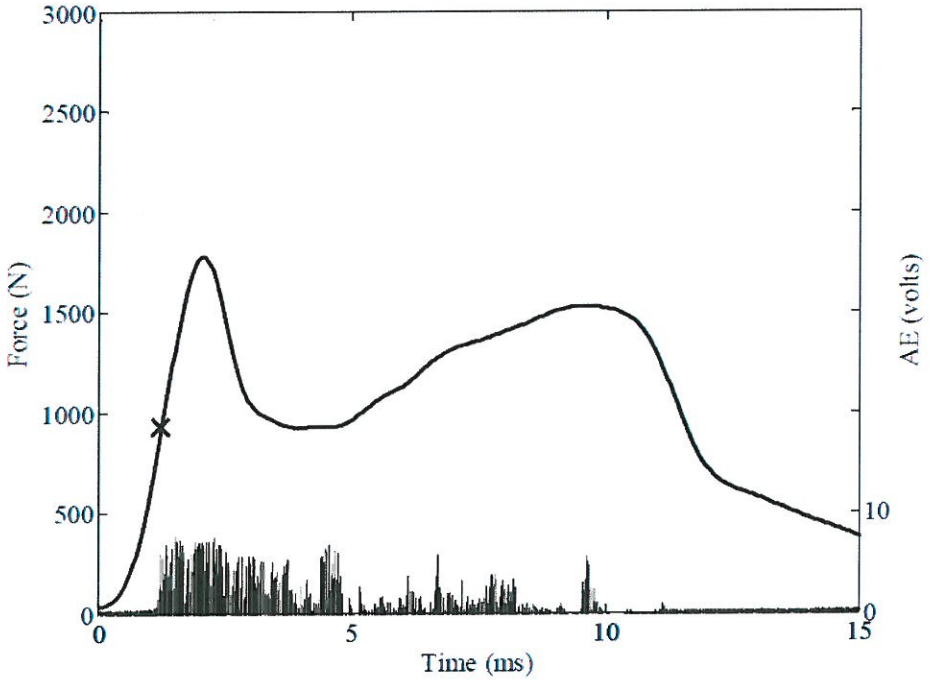

Figure 23: Subject 49 force and acoustic emission response.

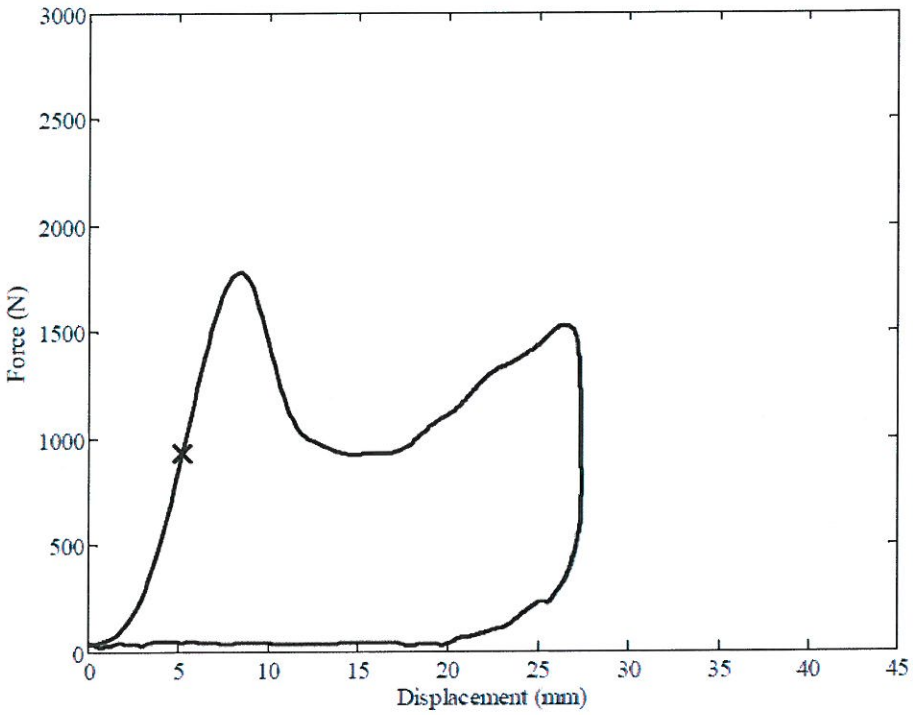

Figure 24: Subject 49 force-displacement response.

The response of the zygoma to lateral impact consisted of deformation of the zygomatic arch, lateral aspect of the zygoma and displacement of the impactor into the maxillary sinus. The displacement of the impactor was calculated for every test by double integrating the accelerometer data. The pre-impact velocity of the impactor was determined using high-speed video. All but one test was used to create a force-displacement corridor for the zygoma impacts using the characteristic average and standard deviation (Figure 25). The single test was removed due to difficulty in assessing the time of contact.

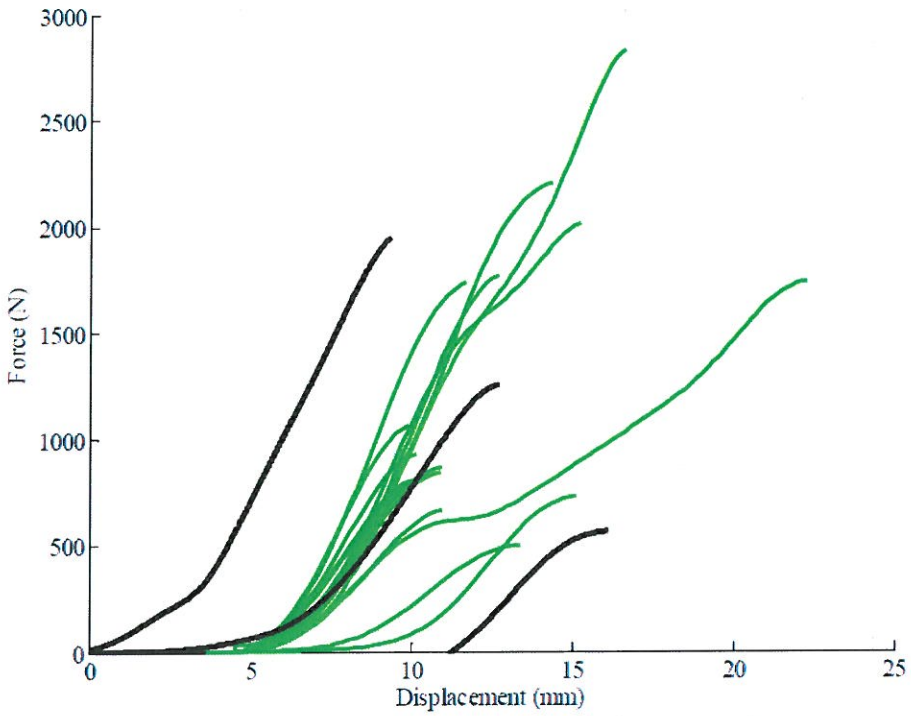

Figure 25: Force displacement response to peak force and corresponding corridors.

The fracture patterns observed during the zygoma impacts was fairly consistent among tests (Figure 26, Figure 27). Medially, the fractures typically propagated along the sture line between the zygoma and frontal process of the maxilla. Laterally, the fracture typically occurred at the zygomatic arch and frontal process.

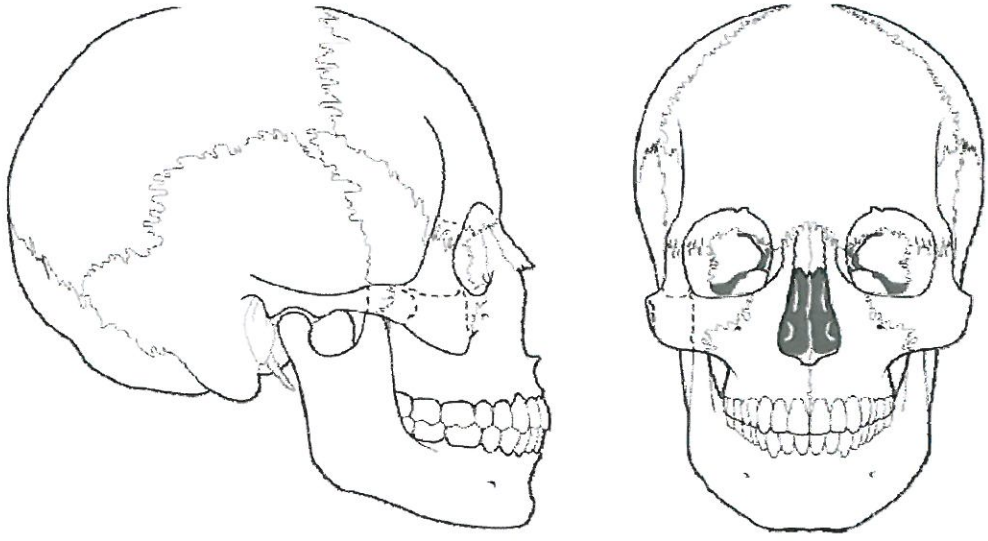

Figure 26: Fracture pattern observed in subject 42.

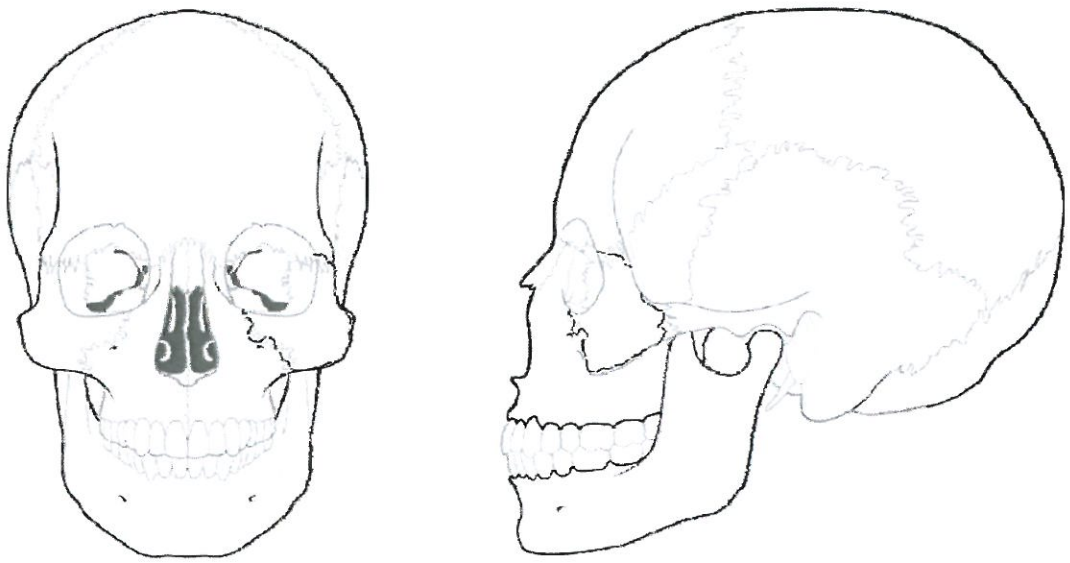

Figure 27: Fracture pattern observed in subject 49.

The risk of fracture was estimated using a Weibull distribution (Table 5) and the Kaplan-Meier non-parametric technique (Figure 28). Since no fracture occurred until a force of 500 N, the Kaplan-Meier model indicates zero risk up to this force. Both models predict similar risk of fracture between 25 and 50 percent, and then diverge slightly thereafter. Subject age was not a statistically significant factor for predicting zygoma fracture. Using the Kaplan-Meier estimate a 50% risk of zygoma fracture occurs at a force between 650 and 700 N.

Table 5: Parameter estimates for Weibull model.

		95% Confidence Interval	
Parameter	**Estimate**	**Lower**	**Upper**
Scale (λ)	3.44E-06	5.86E-08	7.58E-05
Shape (γ)	1.81	1.31	2.50

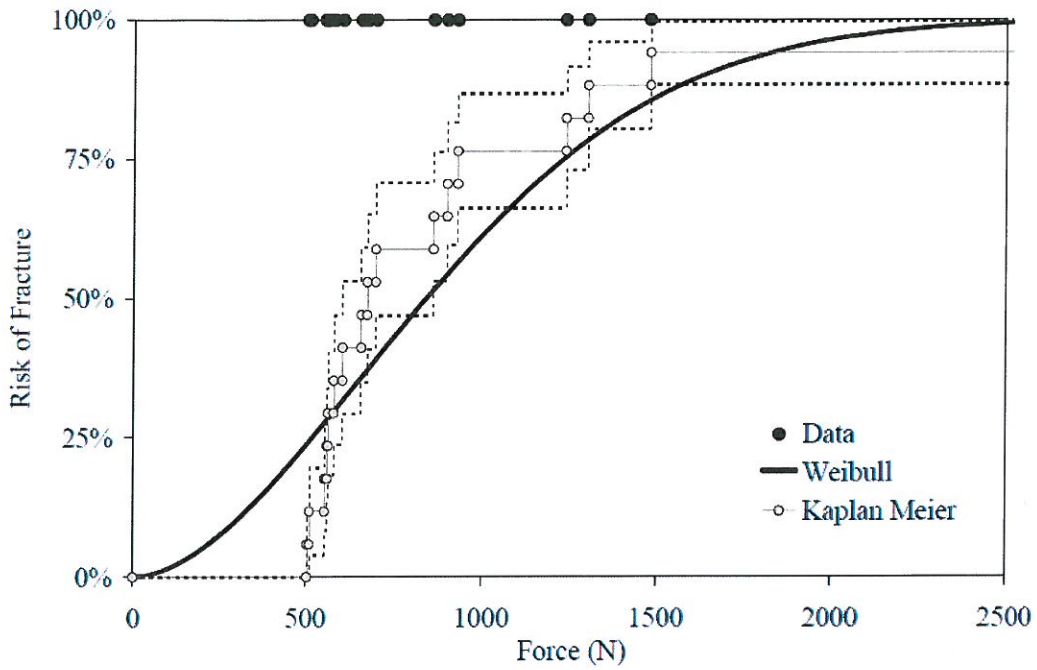

Figure 28: Risk of zygoma fracture due to lateral impact.

NASAL BONE: A total of 19 lateral impact tests were performed using male cadaver specimens (Table 6). The average impact velocity was 2.2 m/s which resulted in energy at impact of 7 to 10 J, with an average of 8 J. The peak force ranged from 76 to 723 N with an average of 368 N. Only one test did not result in fracture, which was the test resulting in the lowest peak force of 76 N. A threshold for the Acoustic Emission (AE) data associated with fracture was set to 5 volts. This threshold was higher than the maximum value of AE recorded during the non-fracture frontal bone tests (0.6 v) performed on the same subjects. The maximum AE measured during fracture producing impacts for the nasal and frontal bone impacts had an average value of 8.1 and 8.7 respectively. The slightly lower value for the nasal bone impacts is consistent with the AE sensor being farther away from the nasal bone than frontal bone impact locations. On average, fracture force was equal to 32% of the peak force achieved during the fracture tests (Figure 29). The peak force achieved during each test did not demonstrate a relationship to the initial impactor energy (Figure 30).

Table 6: Results of lateral nasal bone impacts.

Specimen Number	Impact Velocity (m/s)	Impact Energy (J)	Peak Force (N)	Fracture Force (N)
38	2.2	7.6	355	79
39	2.1	7.0	298	138
40	2.3	8.2	243	102
41	2.1	7.1	271	143
42	2.2	7.4	241	71
43	2.3	8.3	375	114
44	2.5	9.6	352	89
45	2.1	7.0	360	61
46	2.2	7.6	76	-
47	2.1	7.3	253	84
48	2.2	7.6	308	86
49	2.1	6.9	615	138
50	2.4	9.3	397	146
52	2.1	7.2	378	378*
53	2.2	7.4	657	87
54	2.3	8.0	320	320*
55	2.1	6.7	723	410
56	2.1	6.7	356	76
57	2.4	9.3	414	130

* AE data not available

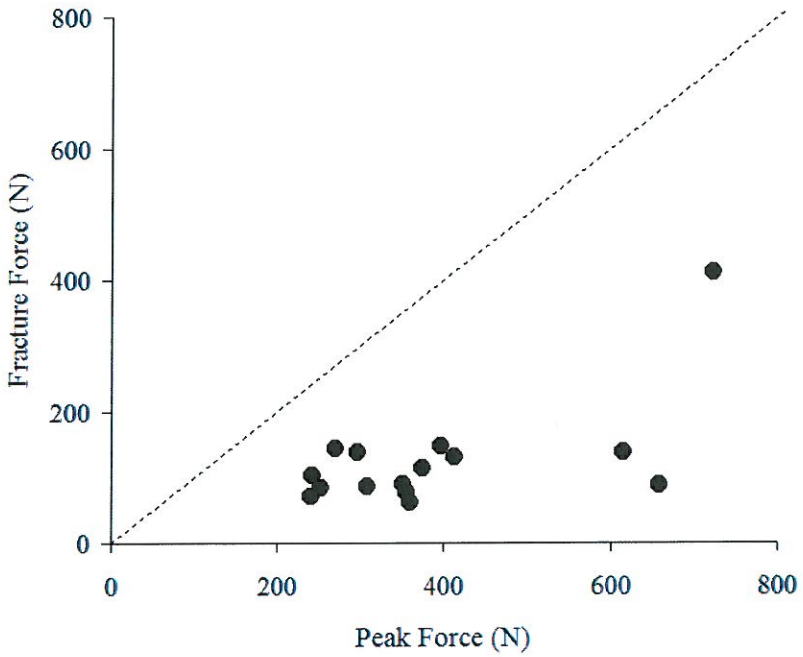

Figure 29: Corresponding fracture and peak forces for lateral nasal bone impacts.

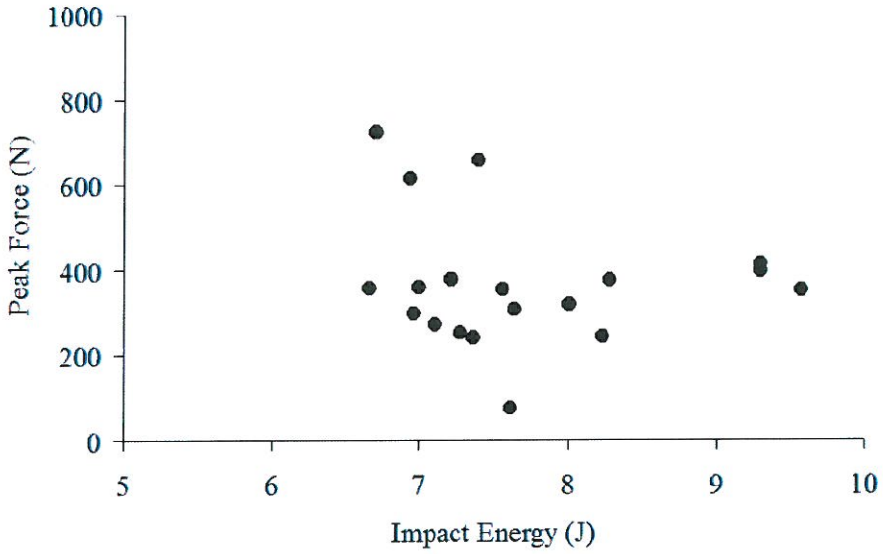

Figure 30: Impactor energy and resulting peak force for all tests.

The response of the nasal structure to the lateral impacts consisted of lateral translation of the nose and a bending of the soft structures in the direction of the impact. The displacement of the impactor was calculated for every test by double integrating the accelerometer data. The preimpact velocity of the impactor was determined using high-

speed video. Using the calculated displacement response and high speed video, tests with inaccurate force-displacement data were identified. These tests were not used for the force-displacement response because initial contact between the impactor and other facial structures of the subject caused the impactor to slow a minute amount. This made it difficult to determine the exact time the impactor struck the nose. Twelve tests were utilized to evaluate the force-displacement response of the nasal bone to lateral impact. The distribution of the force-displacement response was characterized using the characteristic average and its standard deviation (Figure 31).

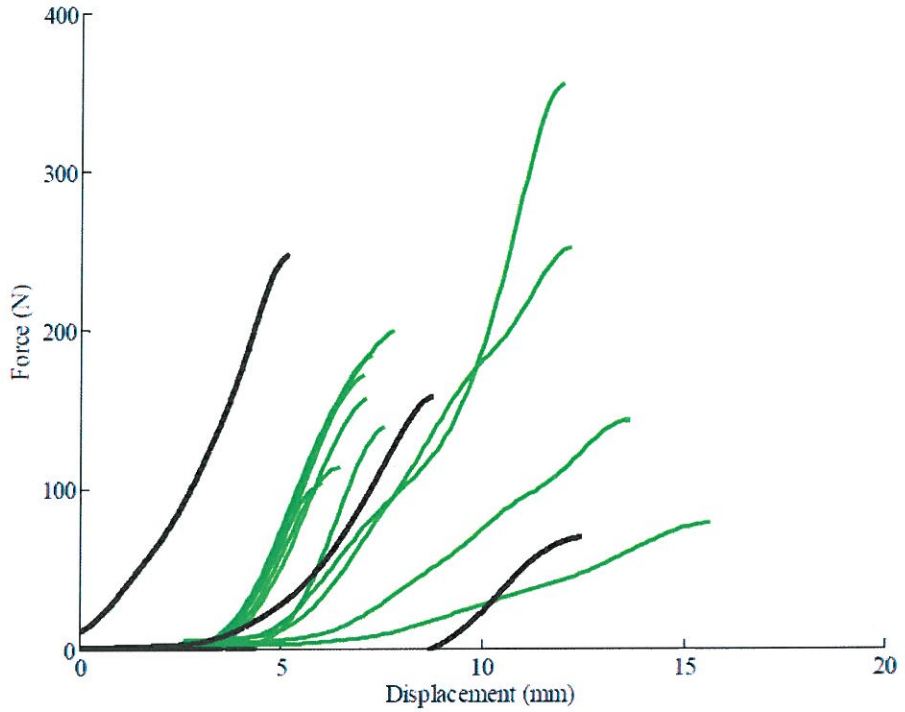

Figure 31: Force-displacement response of lateral nasal bone impacts with corresponding characteristic average and standard deviation.

In 11 of the 19 tests, the fracture force identified by the AE was coincident with a local peak in the force response (Figure 33), while in the remaining tests fracture was identified prior to a single peak in the force response (Figure 32). In tests with a local peak around the fracture force, the difference in magnitude between fracture force and the local peak was 14 N on average. Based on the AE data, fracture occurred fairly early in the event, before the extensive motion of the major structure of the nose. On average, the AE signal began after approximately 4 mm (std dev = 1.2) of impactor travel. In two tests resulting in fracture, AE data were not available; therefore, the peak force was utilized in the survival analysis and treated as a left censored data point. The remaining fracture force values were treated as non-censored values in the survival analyses.

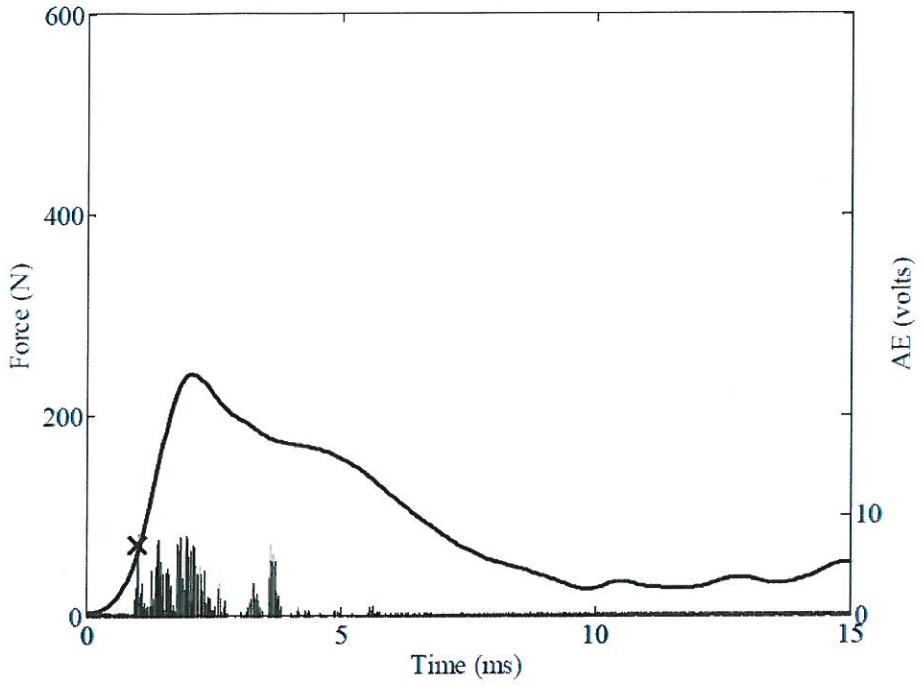

Figure 32: Force and AE response for subject 43.

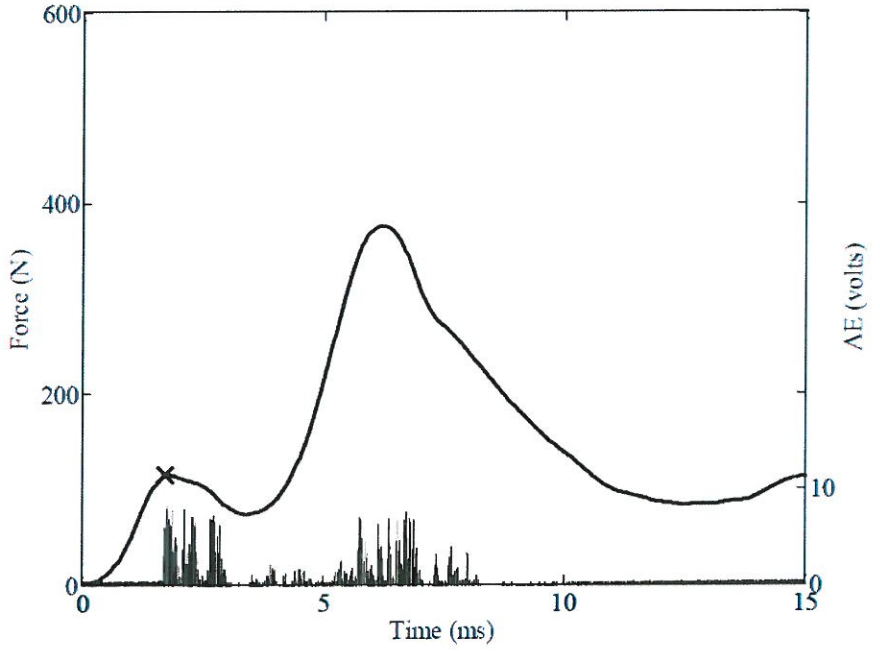

Figure 33: Force and AE response for subject 44.

The risk of fracture was estimated using a Weibull distribution (Table 7) and the Kaplan-Meier non-parametric technique. The Weibull and Kaplan- Meier methods estimated similar values for risk between 30 and 70% risk. Since no fracture was recorded at a force below 61 N, the Kaplan-Meier estimate predicts a risk of zero until this force level is

reached. In order to fit the data the Weibull model must continually increase the risk estimate from zero; therefore, it predicts a higher level of risk at forces less than 61 N (Figure 34). Subject age was not a statistically significant factor in predicting the risk of nasal bone fracture. Based on the Kaplan-Meier estimate, a 50% risk of nasal bone fracture corresponds to an applied force between 90 and 130 N.

Table 7: Parameter estimates for Weibull model.

			95% Confidence Interval	
Model	**Parameter**	**Estimate**	**Lower**	**Upper**
Weibull	Scale (λ)	1.59E-04	1.26E-05	1.16E-03
	Shape (γ)	1.77	1.29	2.42
	Age	1.00	1.00	1.00

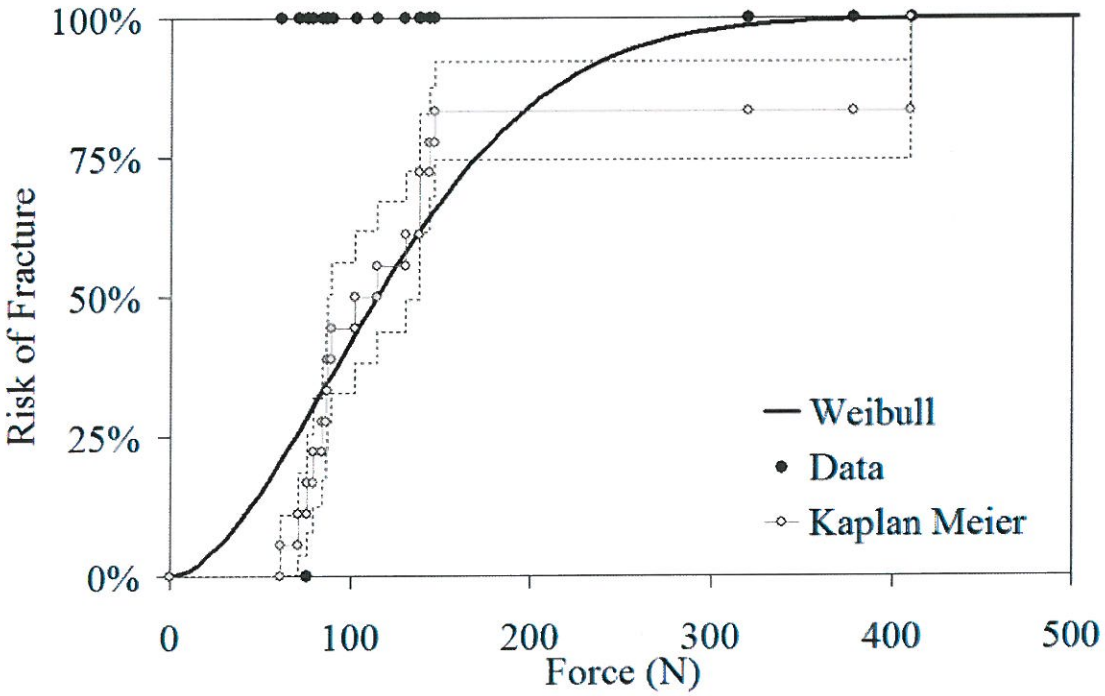

Figure 34: Risk of nasal bone fracture due to lateral impact.

The fracture patterns exhibited by the subjects were fairly consistent. All subjects incurred fractures to the nasal bones and the majority also exhibited a fracture propagating inferiorly along the frontal process of the maxilla. The fracture of the medial aspect of the maxilla mostly occurred on the same side as the impact, (Figure 36) but in some cases the maxilla was fracture on the contralateral side (Figure 35). This suggests that the fracture to the frontal process of the maxilla is due to an avulsion process from forces applied by the nasal structures.

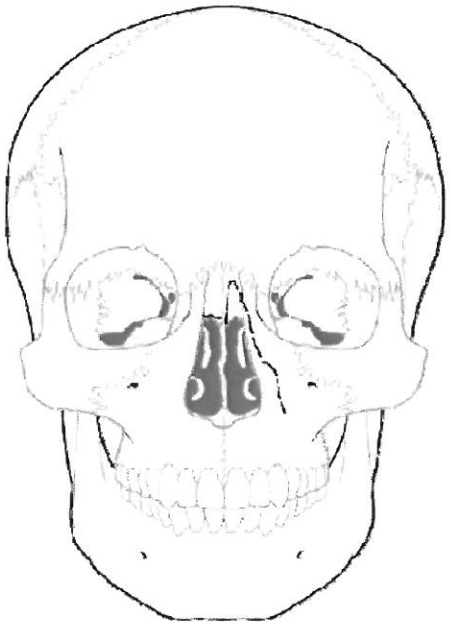

Figure 35: Fracture pattern in subject 43 due to right sided impact shown in Fig. 32.

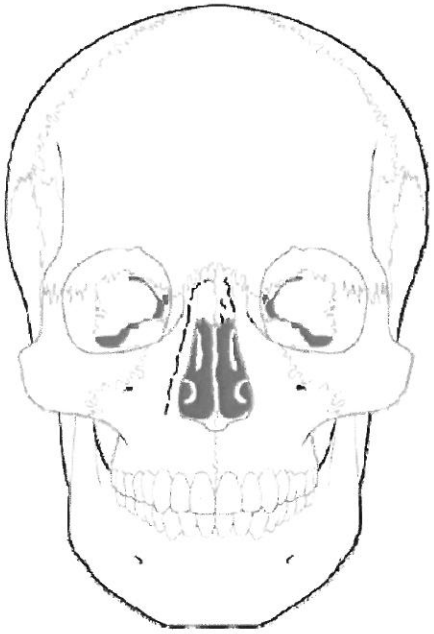

Figure 36: Fracture pattern in subject 44 due to right sided impact shown in Fig. 33.

FOCUS Response: A total of 22 tests were performed on the FOCUS headform to evaluate its response to lateral impact (Table 8). The impactor velocity and, therefore

energy was fairly similar among all tests. The average impactor energy was 7 J with a range of 6.3 to 7.9 J. Five tests at each speed were performed on the frontal bone and zygoma, and one test at each speed was performed on the nasal bone.

Table 8: Results of lateral FOCUS impact tests by impacted region.

Test	Bone	Impact Velocity (m/s)	Impact Energy (J)	Peak Force (N)	Displacement at Peak Force (mm)
1	Frontal	2.00	6.29	1884	9.8
2	Frontal	2.00	6.29	1897	9.6
3	Frontal	2.00	6.29	1860	9.1
4	Frontal	2.00	6.29	1918	8.9
5	Frontal	2.00	6.29	1915	9.4
6	Frontal	2.23	7.86	2237	9.4
7	Frontal	2.23	7.86	2217	9.4
8	Frontal	2.23	7.86	2242	9.3
9	Frontal	2.23	7.86	2253	8.9
10	Frontal	2.23	7.86	2195	9.5
11	Zygoma	2.00	6.29	1349	11.9
12	Zygoma	2.00	6.29	1386	11.3
13	Zygoma	2.00	6.29	1404	11.3
14	Zygoma	2.00	6.29	1352	11.2
15	Zygoma	2.00	6.29	1379	11.5
16	Zygoma	2.23	7.86	1599	14.8
17	Zygoma	2.23	7.86	1637	11.6
18	Zygoma	2.23	7.86	1561	13.7
19	Zygoma	2.23	7.86	1592	11.9
20	Zygoma	2.23	7.86	1602	13.6
21	Nasal	2.00	6.29	765	5.8
22	Nasal	2.23	7.86	844	6.9

The average peak force exerted onto the frontal bone was 2100 N with a range of 1900 to 2250 N. For the nasal bone, the average peak force was 800 N with a range of 765 to 840 N. The average peak force during the zygoma impacts was 1500 N with a range of 1350

to 1640 J. The narrow range in peak force for similar impact severity demonstrates the repeatability of the FOCUS headform.

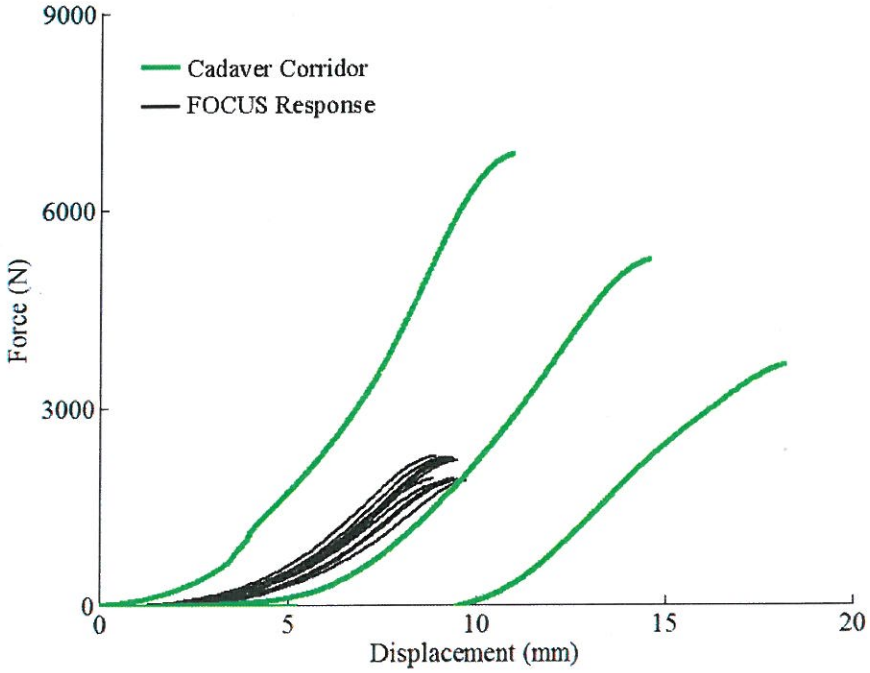

Figure 37: Frontal bone response during FOCUS and cadaver testing.

The force displacement response of the FOCUS headform was plotted against the previously reported cadaver corridors to facilitate comparison. With respect to the frontal bone, the FOCUS response was near the average response of the cadaver specimens (Figure 37). This figure also demonstrates the repeatability of the FOCUS headform during the frontal impacts.

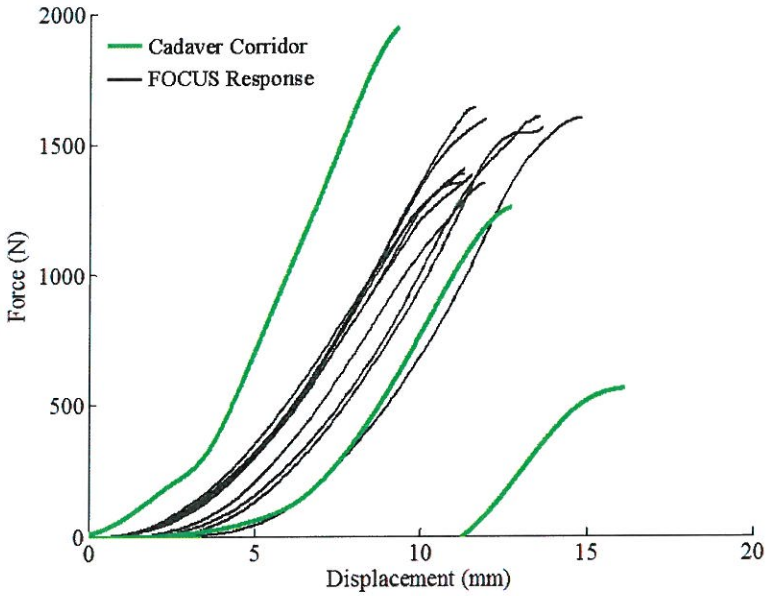

Figure 38: Zygoma response during FOCUS and cadaver testing.

The FOCUS response to lateral zygoma response was similar to the frontal impacts in that they were repeatable and well within the cadaver response corridor (Figure 38). Again, the FOCUS response was slightly stiffer than the average cadaver response; however, it was substantially lower than the higher bound of the cadaver corridor.

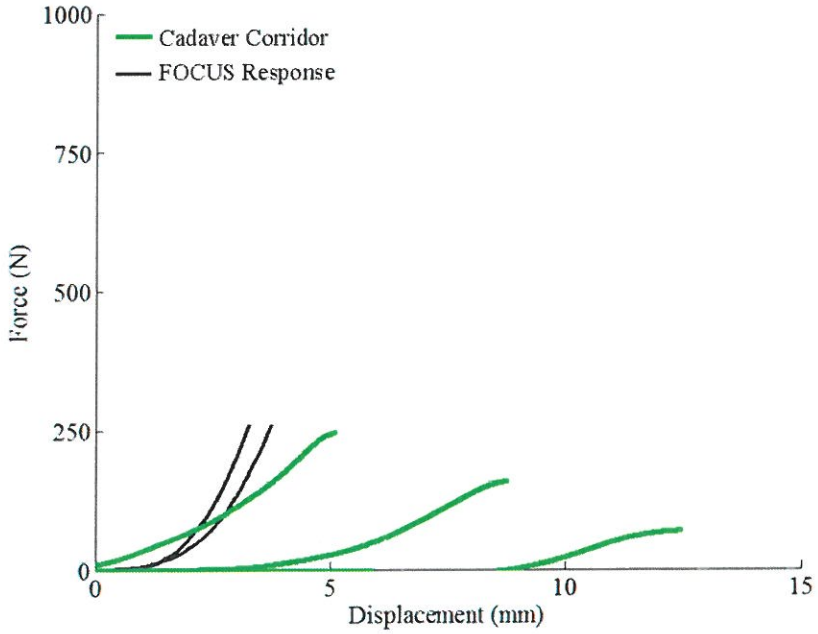

Figure 39: Nasal bone response during FOCUS and cadaver testing.

The response resulting from impact to the nasal structure of the FOCUS headform is compared to that of the cadaver specimens in Figure 39. While the first few mm of displacement are in good agreement with the cadaver data, the FOCUS headform nasal structure demonstrated an overall stiffer response than the cadaver specimens. This response results from the impactor interaction with the FOCUS reaction surface meant to replicate the nasal bone. The relatively thin rubber material covering this area of the nasal bone provides little resistance to the impactor and, therefore, the majority of the impact is against the stiff underlying structure. This results in a conservatively high measurement for an impact to the nasal structure on the FOCUS headform.

FRONTAL BONE: This study is a continuation of previously published work on the response of the frontal bone to Anterior-Posterior (AP) impacts (Cormier, 2010). The previous study was performed using the exact methods and impactor and produced similar peak forces with respect to impact severity (Figure 40). Also of interest is that the force at fracture onset identified using AE data was similar in both studies. The average fracture force in the current study was 2119 N (SD: 1032) and during the AP testing, the average fracture force was 1982 (SD: 765).

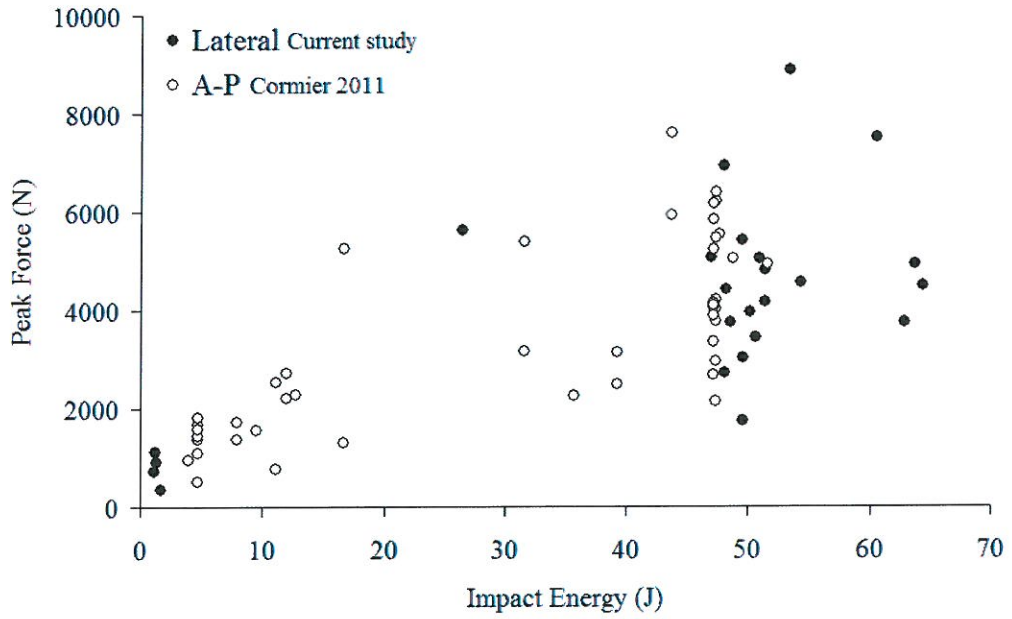

Figure 40: Peak forces produced during current and previous study by impact direction on frontal bone.

The peak forces generated in this study are also similar to those of previous studies utilizing a similar impactor size (with padding) in the AP direction (Nahum, 1975; Nahum

1968) (Figure 41). Two of the non-fracture tests in the current study exhibited the highest peak force which is consistent with the ability to support more force if fracture does not occur. As a result of the testing performed by Nahum *et al.* (1968, 1975), they proposed a tolerance of the frontal bone to A-P impacts of 3560 to 7120 N. Based on the non-parametric risk curve developed in the current study, these forces correspond to a 74 to 99% risk of fracture. The proposed tolerances are on the upper end of the risk curve because they are based on peak force and not the force at fracture onset. Also, the force to cause fracture in the current study may be lower due to the lack of padding compared to the Nahum *et al.* studies.

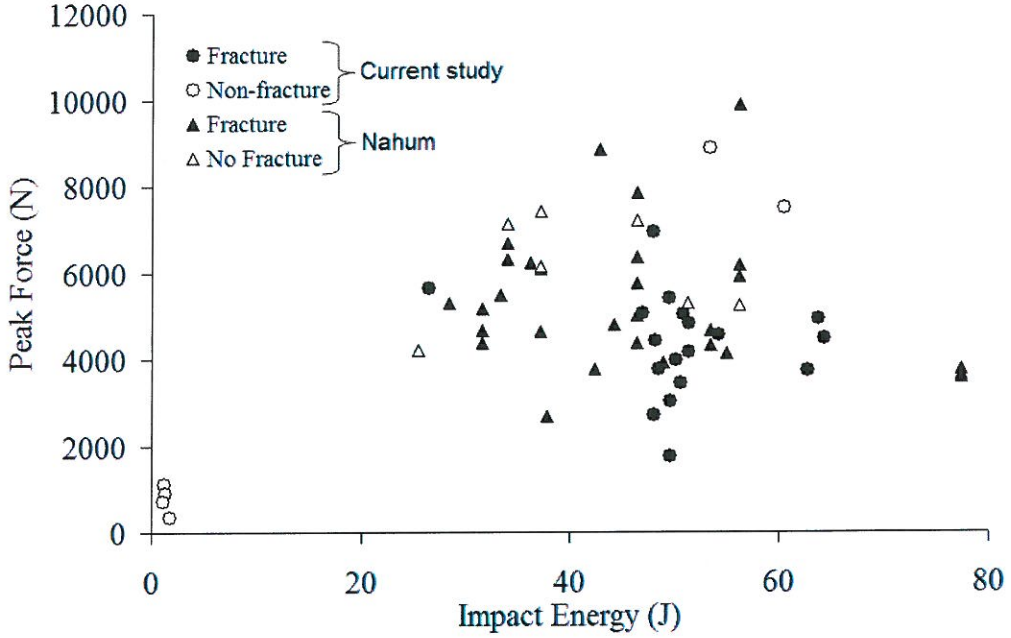

Figure 41: Impactor energy and peak force for current previous studies.

The Bermond *et al.* (1999) study which used a cylindrical impactor to perform oblique (30o) impacts to the frontal bone measured average peak forces of 4050 N during non-impact producing tests. The risk curve created during the current study suggests that force level represents a fracture risk of 82%. This suggests that the cylindrical impactor may present a less aggressive impacting surface than the flat, rounded shape used in the current and the Nahum *et al.* studies. These results are consistent with those of Allsop *et al.* (1988) who found an average force of fracture onset of 4800 N when performing A-P impacts using a cylindrical impactor. The higher force to fracture is likely due to the cylindrical impactor and the A-P direction distributed the force across a greater area on the frontal bone than the oblique impacts.

ZYGOMA: The current study provides a statistical relationship between impactor force and risk of zygoma fracture for lateral impacts. Additionally, the force-displacement response of the zygoma to lateral impact has been described using the characteristic average. Some comparison can be made to previous studies on the impact tolerance of the zygoma (Figure 42). Caution should be used when evaluating the risk of fracture however, since the previous work is limited to peak force while the current study utilized acoustic emission sensors to identify the force at fracture onset. The impacts in the current study were performed at slightly higher energies than previous work; however the peak force achieved during each study was similar. This demonstrates that lateral zygoma impacts are a load-limiting event due to the loss of integrity to the underlying structures.

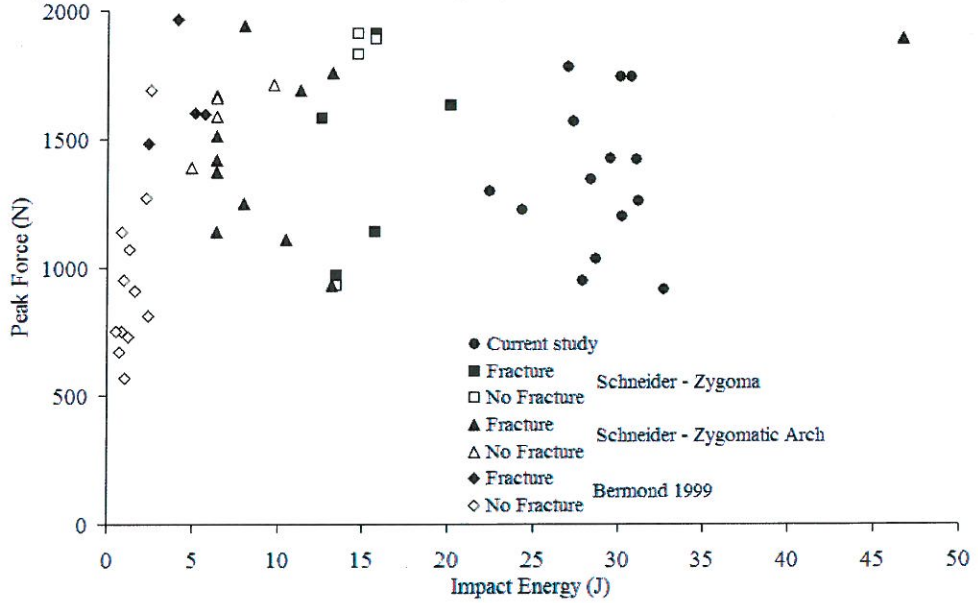

Figure 42: Peak force achieved in zygoma impacts during current and previous studies.

The previous work by Schneider et al. (1972) consisted of oblique impacts to the zygoma using a similar sized impactor with nickel padding. Their study produced average peak forces of 1640 and 1680 N for the no-fracture and fracture tests respectively. According to the Kaplan-Meier estimates of the current study, these forces correspond to a fracture risk of 88 to 99%. The high risk without fracture is likely due to the oblique nature of the Schneider impacts which may be a stronger loading direction for the zygoma. Additionally, this results from the conservative nature of using acoustic emission to determine fracture onset since this will occur with little change in the structural integrity of the bone (Rajachar, 1999). Age was not found to be significantly correlated with the risk of fracture for the lateral zygoma impacts.

NASAL BONE: This study expands on the current knowledge nasal bone tolerance by performing a series of lateral impacts to the nasal bone using a flat round impactor. The average impactor energy was 8 J (Stand. Dev. = 1) resulting in average peak forces of 370 N (S.D. = 120). A total of nineteen tests were performed, all but one resulted in fracture of the nasal bone. Force at the onset of fracture was identified using an Acoustic Emission (AE) sensor attached to the frontal bone. The average force at fracture onset was 122 N (S.D. = 82). This is significantly lower than the average fracture force achieved during Anterior-Posterior (AP) impacts performed in a previous study (Cormier, 2010). The previous study utilized the same impactor and methods as the current study and the average force at fracture was 664 N (S.D. = 434). Peak forces achieved during the previous study were also significantly higher than the lateral impacts (Figure 43). This results from the facial structures posterior to the nasal bones that will continue to provide support after the nasal bones fracture.

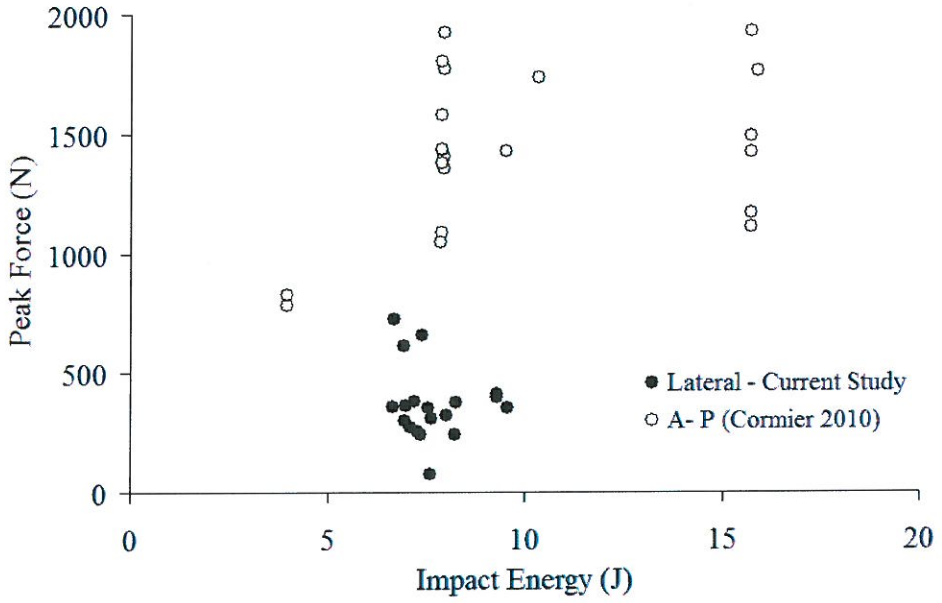

Figure 43: Peak forces achieved during lateral and A-P nasal bone impacts.

The tolerance of the nasal bone was estimated using a Weibull parametric model and the Kaplan- Meier estimate which is a non-parametric estimate. Both methods estimated similar risk values near the 50% point, but deviate toward the lower end of fracture force. Considering the geometry of the nasal bones, it is expected that its tolerance would be lower in the lateral direction than the AP direction. Therefore, it is likely that oblique impacts to the nasal bones would result in fracture at lower forces than a purely AP directed impact.

The fracture patterns observed during this study were interesting in that direct impact to the frontal process of the maxilla was not necessary to cause fracture. Also, the occurrence of fracture on the frontal process opposite the impacted side demonstrated the avulsion mechanism of created these fractures. This demonstrates that the facial fracture patterns should be examined carefully when attempting to determine the direction of impact.

FOCUS RESPONSE: Twenty-two lateral impact tests performed on the FOCUS headform to relate the FOCUS frontal bone, zygoma, and nasal bone response that measured from cadaver tests. The results of this test series are consistent with previously reported force-displacement data obtained during frontal impacts. The frontal bone demonstrated a repeatable response that was similar to the average response exhibited by the cadaver specimens. The nasal bone demonstrated a repeatable response; however it produced conservatively high force response for a given displacement when compared to the cadaver data. The zygoma region of the FOCUS headform demonstrated a biofidelic response that was similar to the average response of the cadaver specimens. Overall, the FOCUS headform produced a biofidelic and repeatable response for lateral impact to the frontal bone, zygoma, and nasal bone.

KEY RESEARCH ACCOMPLISHMENTS:

- For blunt lateral impact, biofidelity corridors were generated for:
  - Frontal bone
  - Zygoma
  - Nasal bone
- For blunt lateral impact, injury risk curves were generated for:
  - Frontal bone
  - Zygoma
  - Nasal bone
- For blunt lateral impact, the biofidelity of the FOCUS headform was assessed for:
  - Frontal bone
  - Zygoma
  - Nasal bone
  -

REPORTABLE OUTCOMES:

Reports

- Rowson S, Cormier J, Duma S. Interim Report: Injury Criteria for Lateral Facial Fracture. CIB Report 2010-013.
- Rowson S, Cormier J, Duma S. Interim Report 2: Injury Criteria for Lateral Facial Fracture. CIB Report 2011-012.

- Rowson S, Cormier J, Duma S. Final Report: Injury Criteria for Lateral Facial Fracture. CIB Report 2012-011.

Presentations

- Rowson S, Facial Fracture and Injury Risk Functions for Lateral Impact to the FOCUS Headform. Fort Detrick, September 27, 2011.

Future Journal Publications

- Tolerance of the frontal bone to lateral blunt impact. Journal of Biomechanical Engineering.
- Tolerance of the zygoma to lateral blunt impact. Journal of Biomechanical Engineering.
- Tolerance of the nasal bone to lateral blunt impact. Journal of Biomechanical Engineering.
- Biomechanical response corridors of the human face to lateral impact and corresponding biofidelity of the FOCUS headform. Journal of Aviation, Space, and Environmental Medicine.

CONCLUSION: A series of 64 drop tests were performed to evaluate the frontal, zygoma, and nasal bones of 20 PMHS heads were fractured while collected data quantifying impact force and acoustic response. Biofidelity corridors and injury risk functions were developed for blunt lateral impact to the frontal bone, zygoma, and nasal bone. A series of 22 matched tests were performed to assess the biofidelity of the FOCUS headform to blunt lateral impact. Overall, the FOCUS headform produced a biofidelic and repeatable response for lateral impact to the frontal bone, zygoma, and nasal bone. Future use of these analyses will aid design engineers in optimizing the development of enhanced face and eye protective equipment.

REFERENCES: Allsop, D., Warner, C., Wille, M., Schneider, D., and Nahum, A., 1988, "Facial Impact Response – a Comparison of the Hybrid 3 Dummy and Human Cadaver," Society of Automotive Engineers, SAE No. 881719.

Bermond, F., Kallieris, D., Mattern, R., Ramet, M., Bouquet, R., Caire, Y., and Voiglio, E., 1989, "Human Face Response at an Angle to the Fore-Aft Vertical Plane Impact," eds., Proceedings of the IRCOBI, pp. 121-32.

Cantor, A. B., 2003, Analysis Techniques for Medical Research, SAS Press, Cary.

Cormier J, Bisplinghoff J, Duma S. Fracture Tolerance Thresholds of Human Facial Bones Subjected to Blunt Impact. CIB Report 2008-030.

Cormier, J., Manoogian, S., Bisplinghoff, J., Rowson, S., Santago, A., Mcnally, C., Duma, S., and Bolte, J. T., 2011, "The Tolerance of the Frontal Bone to Blunt Impact," J Biomech Eng, 133:021004.

Cormier, J., Manoogian, S., Bisplinghoff, J., Rowson, S., Santago, A., Mcnally, C., Duma, S., and Bolte Iv, J., 2010, "The Tolerance of the Nasal Bone to Blunt Impact," Ann Adv Automot Med, 54 (pp. 3-14).

Kleinbaum, D., and Klein, M., 2005, Survival Analysis: A Self-Learning Text, Statistics for Biology and Health, Springer Science, New York.

Lessley, D., Crandall, J., Shaw, G., Kent, R., and Funk, J., 2004, "A Normalization Technique for Developing Corridors from Individual Subject Responses," Society of Automotive Engineers, 2004-01-0288.

Nahum, A. M., 1975, "The Biomechanics of Facial Bone Fracture," Laryngoscope, 85 (1), pp. 140-56.

Nahum, A. M., Gatts, J. D., Gadd, C. W., and Danforth, J., 1968, "Impact Tolerance of the Skull and Face," eds., Proceedings of the 12th Stapp Car Crash Conference, New York, October 22-23, pp. 302-316.

Rajachar, R. M., Chow, D. L., Curtis, C. E., Weissman, N. A., and Kohn, D. H., 1999, "Use of Acoustic Emission to Characterize Focal and Diffuse Microdamage in Bone," Acoustic Emission: Standards and Technology Update, ASTM STP 1353, Ed. Vahaviolos SJ, ASTM.